TALLINN UNIVERSITY OF TECHNOLOGY

SCHOOL OF ENGINEERING

Department of Materials and Environmental technology

KESTERITE SOLAR CELLS FOR EXTRATERRESTRIAL APPLICATIONS

KESTERIIT PÄIKESEPATAREID KASUTAMAKS KOSMOSE KESKKONNAS

MASTER THESIS

Student: Levan Chikviladze

Student Code: 184649KAYM

Supervisors: Dr. Kaia Ernits; Dr. Taavi Raadik;

Tallinn 2020

AUTHOR'S DECLARATION

Hereby I declare, that I have written this thesis independently.

No academic degree has been applied for based on this material. All works, major viewpoints and data of the other authors used in this thesis have been referenced.

"26" May 2020

Author: Levan Chikviladze

/signature /

Thesis is in accordance with terms and requirements

"26" May 2020

Supervisor: /electronically signed/

/signature/

Accepted for defence

"26" May 2020.

Chairman of theses defence commission: Prof. Malle Krunks

/name and signature/

DEPARTMENT OF MATERIALS SCIENCE

THESIS TASK

Student: Levan Chikviladze, 184649KAYM

Study programme: KAYM09/18 – Materials and Processes for Sustainable Energetics

main speciality: Processes for Sustainable Energetics

Supervisor (s): Researcher, Dr. Taavi Raadik, 56491983

Researcher, Dr. Kaia Ernits, 5160819

Thesis topic:

KESTERITE SOLAR CELLS FOR EXTRATERRESTRIAL APPLICATIONS

KESTERIIT PÄIKESEPATAREID KASUTAMAKS KOSMOSE KESKKONNAS

Thesis main objectives:

1. Research existing technologies and solutions associated with space photovoltaics
2. Analyze the environmental characteristics of the moon in frames of possible hazards and degradation mechanisms for solar cells
3. Accordingly design an experimental procedure to investigate the performance of crystalsol's CZTSSe monograin solar cells in the lunar environment

Thesis tasks and time schedule:

No	Task description	Deadline
1.	Theoretical research	01.09.19
2.	Experimental procedures	01.02.20
3.	Analysis and discussion of the results; Additional tests;	01.05.20

Language: English **Deadline for submission of thesis:** "26" May 2020a

Student: Levan Chikviladze "26" May 2020a

/signature/

Supervisor: Dr. Taavi Raadik /electronically signed/ "26" May 2020a

/signature/

Co-Supervisor: Dr. Kaia Ernits /electronically signed/ "26" May 2020a

/signature/

Head of study programme: Dr**.** Sergei Bereznev ".....".....201.a

/signature/

Table of Contents

Preface

The following thesis “Kesterite Solar Cells for Extraterrestrial Applications”, the basis for which stemmed from the ongoing multidisciplinary researches and experiments looking for novel photovoltaic materials applicable for extraterrestrial conditions, has been created in collaboration with crystalsol GmbH at Tallinn University of Technology.

As the scientific community sets its sights on getting back to the frontier of vigorous exploration of space, testing advanced solar energy technologies adapted to a wide range of environmental characteristics to power various missions has become one of the most crucial pieces stages of the process. This work is a detailed investigation, theoretical as well as practical, of kesterite – CZTSSe ($CuZnSn(S, Se)_4$) monograin solar cells for the applicability in the lunar environment.

The project was initially undertaken at the request of crystalsol GmbH, in cooperation with which vast theoretical research was conducted, followed by a multistage experimental procedure carried out in the laboratories of TalTech with the samples provided by the company.

I would like to thank Kaia Ernits and Taavi Raadik for the supervision and guidance during the project. Also, express special gratitude to Raavo Josepson, Maarja Grossberg, Marit Kauk- Kuusik and Valdek Mikli for providing the facilities necessary to carry out the experiments throughout the research.

This work was supported by the European Regional Development Fund, Project TK141 and Mobilitas Pluss Returning Researcher Grant MOBTP131.

List of Abbreviations and Symbols

LEO – Low Earth Orbit

GEO – Geostationary Orbit

NASA – National Aeronautics and Space Administration

LILT – Low Intensity Low Temperature

IMM – Inverted Metamorphic Multi-junction

SBT – Semiconductor Bonded Technology

MISSE – Materials International Space Station Experiment

GCR – Galactic Cosmic Rays

SPE – Solar Particle Events

PERL – Passivated Emitter with Rear Locally diffused

CZTS – Cu_2ZnSnS_4

CZTSSe – $Cu_2ZnSn(S,Se)_4$

GaAs – Gallium Arsenide

CdTe – Cadmium Telluride

InP – Indium Phosphide

HES-IBF – High Efficiency Silicon – Integrated Bypass Function

MSC – Minimum Sample Count

GmbH – Company with limited liability (German)

TFC – Transparent Front Contact

Introduction

On April the 25th, 1954 Bell Labs – Industrial research and scientific development company, demonstrated the first practical silicon solar cells and announced significant increase in the output of the device, the effect of which had been first observed back in the first half of the 19th century. On that occasion the demonstration involved powering a toy Ferris wheel and a radio transmitter, which in the span of astounding 4 years evolved into a first ever solar powered spacecraft – Vanguard 1, launched by the United States in 1958. The satellite, which was small enough to be held in one hand, carried a few silicon cells, altogether delivering less than 1 watt. This occasion demonstrated the effectiveness of the solar cell in space, immediately followed by expanded applications, researches and advancements for the extraterrestrial as well as terrestrial use[1][2][3].

Up to today and beyond solar cells are considered as one of the most effective electric power sources for extraterrestrial applications. These include interplanetary and deep-space exploration, satellites at LEO and GEO for meteorology, communication and broadcasting. Space exploration is generally accepted as one of the major stimulators of advances in science and technology, and photovoltaics is not an exception. High potential of solar energy for future missions and experiments, has motivated the entire scientific workforce to get better at harnessing it, by improving the conversion efficiency, increasing the lifespan, enhancing the environment-specific resistance and mass-cost-energy ratio of the solar cells.

The applicability of a given photovoltaic system for a given mission greatly depends on its characteristics. For instance, according to NASA[4], future solar powered planetary science missions are classified as follows -

- **Outer planet missions** – Planets outside the asteroid belt. Namely, gas giants Jupiter and Saturn and ice giants Uranus and Neptune. In this case, solar cells would have to operate in extremely low temperature and low solar irradiance conditions, which practically makes the usage of Radioisotope thermoelectric generators instead more viable. However, NASA's Juno mission, which in 2016 broke the solar power distance record operating at 793 million kilometers and becoming the most distant solar powered machine, proved photovoltaics still somewhat viable even for outer planet missions. Environmental considerations for these kinds of missions also involve long lifespan, reliability and radiation resistance[4].
- **Inner planet missions** – Venus and Mercury, which pose completely different challenges for the photovoltaic systems, manly connected with extremely high-temperature and high solar intensity environment. Additionally, in case of Venus specifically, low solar irradiance, acidic

and corrosive environments are also significant factors, that needs to considered which affect the solar cell performance[4].

- **Mars mission concepts** – Even though solar cells operating on the surface of Mars have been proved to have less implications, several circumstances still need to be taken into account. Namely, sufficient efficiency of the photovoltaic modules, capability of operating under Mars-specific spectral conditions (towards the Red part of the spectrum), removal of the dust, low-mass, ease of deployment and operation of the systems[4].
- **Small body mission concepts** – Dwarf planets, comets and asteroids. Requirements for the solar energy systems include capability to operate in LILT (Low intensity, low temperature) conditions, low mass, low storage volume, high power output and voltage[4].

Space solar cell development has gone through several stages. In the early days the technology was based on single crystal, polycrystal and amorphous Silicon, which was caused by relatively high efficiency of the solar cells accompanied by comparatively low price of the technology. The existence of alternative materials was widely known and accepted during this period as well, however due to certain shortages, especially price and problems with volume production, these technologies took decades to be finally implemented. GaAs – the successor of silicon, for example, demonstrating critical advantages over the silicon (direct band gap closer to the optimal band gap value of 1.34 eV - 1.44 eV opposed to 1.1 eV that of silicon , higher electron mobility, better performance in high temperature environment), however it was around ten times more expensive than predecessor. It was the reason why no earlier than 1990 did GaAs experience sharp rise in mass production for space applications, accompanied by reasonable decrease in the price of the material, advances in the III-V solar cell technology and increasing on-board power and life-cycle requirements in the growing satellite industry. Through the late 1990s and the first decade of the 21st century GaAs in turn evolved from single junction to dual and triple junction devices. Nowadays, these multijunction solar cells are considered the technology of choice for space applications due to their resilience to radiation, tolerance to extreme temperature gradients, small density of defects and recombination centers, accompanied by advanced conversion efficiencies mentioned above. Furthermore, as far as multijunction cell technology is concerned, NASA reports very bright and interesting future demonstrating conversion efficiencies close to 40% under AM0 condition. Supported and funded multidirectional development of high-efficiency solar cells include 1) Dilute nitride, 2) Inverted metamorphic multi-junction (IMM), 3) Semiconductor wafer bonding (SBT) and 4) Upright metamorphic technologies, noteworthy improvements of which are predicted in the near future – ranging from 1 to 10 years depending on the particular technology. It is worth mentioning, however, that IMM and SBT cell already demonstrate conversion efficiencies approaching 35%[4][5][6].

On the other hand, novel photovoltaic materials are also being actively tested for the space applications. For instance, in frames of Materials International Space Station Experiment (MISSE)- 12, which alongside other MISSE missions, incorporates long-term exposure of different materials of interest to the hostile space environment, five novel types of photovoltaic devices are being extensively tested – Texture carbon nanotube – based cells; Perovskite cells; CZTS cells; low – cost organic cells; Traditional silicon – based cells; [7]–[9].

Unlike high efficiency multi-junction devices, these cells are advantageous on the different end of the spectrum. Particularly - Textured carbon nanotube-based ones are designed in 3D textured fashion to capture the light regardless of the incident angle; Organic solar cells demonstrate a very attractive weight to power ratio theoretically allowing to get hundreds of kilowatts per kilogram of the active material – a crucial property for space applications; CZTS solar cells are considered one of the most promising next-generation solar devices due to the abundance and low cost of the constituent materials, ease of manufacturing and high absorption coefficient; In all cases, the research serves the same purpose – investigate the performance and the degradation mechanisms of the devices in space conditions, thus determining whether a respective photo–absorber can efficiently be used in space[10].

According to William Gerstenmaier of the Human Exploration and Operations Directorate at NASA headquarters, exploring the Moon and its resources will ultimately translate toward human missions to mars, which confirms that not only will the lunar base serve for the habitation and investigation of the Moon, but it also will provide a power and propulsion element – a foundation for exploration further into the solar system. As the scientific community sets its sights on human presence and exploration of deep space, the moon is emerging as the frontier for the future planetary endeavors. The idea of a lunar outpost allowing for a sustained presence on the Moon dates to the 20th century, when this idea was conceptualized into several designs of a lunar habitat. Thorough studies have been conducted since the Apollo missions to evaluate the conditions, boundaries and limitations of expanding human presence to the Moon. The lunar environment possesses several unique and crucial characteristics that significantly affect these. Therefore, analyzing, designing and constructing a lunar base is a multi-variable engineering problem. Considerable scientific advantages of the south polar location for the lunar base have been brought forward. Particularly, as far as solar energy is concerned as possible source for powering lunar base, certain areas of the south pole of the Moon, near the Shackleton crater, are extensively exposed to the direct sunlight – over 200 Earth days of continuous illumination and best location for lunar outpost[11]–[15].

Aim of the study was to evaluate kesterite monograin layer solar cell suitability for space applications. Current thesis will focus solely on CZTS solar cells and analyze extensive experimental process designed to investigate and estimate the behavior of these devices in lunar conditions by testing kesterite monograin layer solar cells in simulated lunar environment. Besides, prior to this, a substantial theoretical research will be conducted. Additionally, topic of the thesis was triggered by the remarkable interest of European Space Agency to the monograin layer solar cell technology to be used for powering future lunar outpost.

1. Theoretical background

1.1. CZTS solar cells

As much as thin-film solar cell technologies have gained popularity over the years, significant issues have also emerged that hinder further development of these devices. Particularly, high cost, material availability and mass production capability are the biggest ones. All mainstream, commercially successful technologies including CdTe, $CuInS_2$(CIS), $CuInGaSe_2$(CIGS) and GaAs share these restrictions, especially the usage of limited/toxic materials. Therefore, the Copper Zinc Tin Sulfide (CZTS), Copper Zinc Tin Selenide (CZTSe) and their solid solution Copper Zinc Tin Sulfo-Selenide (CZTSSe), consisting of earth abundant, non-toxic, significantly cheaper materials, thus solving these issues, have emerged as one of the most potent and promising absorber layers for new-generation thin-film solar cells[16]–[18].

Moreover, having the Kesterite (Fig. 1) structure, these semiconductors possesses a suitable band gap from 1.0 eV for CZTSe to 1.5 eV for CZTS. Bandgap value is possible to tune in that range 1-1.5 eV by variating Sulfur-Selenium ratio in the CZTSSe solid solution, allowing the maximum theoretical efficiency of 33.8% at bandgap value of 1.34 eV under AM1.5 illumination. Kesterite material is strong absorber with relatively large absorption coefficient of over 10^4 cm^{-1} in the wavelength ranges of 350-1000 nm and necessary p-type conductivity. Over the years, due to these crucial assets, the development of this absorber material has gained considerable momentum, which as mentioned above, has resulted in increased interest from the scientific society including space agencies like NASA and ESA. First ever published kesterite solar cell record efficiency was as low as 0.66% in 1997[19], having gained a lot of attention lately, continuous efforts have led to constant improvement of the technology, already surpassing the efficiency milestone of 10% and having a very bright outlook for the future. Up to date, the reported record efficiencies for CZTS, CZTSe and CZTSSe solar cells are 11.0%[20], 11.6%[21] and 12.6%[22], respectively. In order to fabricate CZTS thin films there are numbers of different techniques, the most spread ones are chemical bath deposition; electrodeposition; co-evaporation and co-sputtering[23]; Nevertheless, is worth to mention also monograin layer solar cell with CZTSSe absorber reaching efficiency of almost 10% by crystalsol[24].

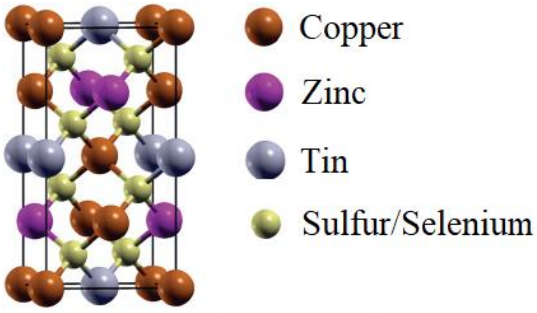

Fig. 1. Kesterite structure of CZTSSe. Body-centered tetragonal with c≈2a, consisting of two alternating cation layers each containing Cu and Zn or Cu or Sn[18].

1.2. Lunar environment and some characteristics

The Moon holds hostile environment to the humans and for solar cell operation. The Moon's surface gravity is only one-sixth of that of the Earth resulting in much lower escape velocity and its inability to maintain a significant atmosphere. Contrary to the widely adopted belief, the Moon happens to have an atmosphere so thin though, that it technically is referred to as an exosphere. There are estimated to be around 10^6 molecules per cubic centimeter, possibly consisting of small portions of argon-40, helium-4, oxygen, methane, nitrogen, carbon monoxide and carbon dioxide[25]. Even at the landing site with the presence of exhaust from the rocket that obviously degrades the ambient high-vacuum environment, the Apollo mission still measured the pressure of 10^{-8} Torr. This parameter has been observed to fluctuate during tremendous daily swings in surface temperature. For instance, the pressure was 10^{-12} Torr shortly after sunset, fluctuating to 10^{-10} Torr due to releases of gas or rapid warming of the surface. The moon rotates on its axes in about 28 days with the daytime on one side lasting about 14 days. Under sunlight the surface temperature may reach 127° C, while in the shade it might fall to minus 173° C, however much lower temperatures have also been observed on the poles[25]–[27]

In terms of damaging effects to humans and electronic devices, lunar radiation environment is one of the most important and influential factors. Due to the complete absence of atmospheric and magnetic shielding, continuous exposure to intense ultraviolet radiation, galactic cosmic rays (GCR) and common solar particle events (SPE) are observed. To put it into perspective, the annual exposure cause by galactic cosmic rays on the surface of the Moon is approximately 110 mSv during solar minimum and 380 mSv during solar maximum, whereas the portion of GCR in the annual dose of natural ionizing radiation of 2.4 mSv is roughly 0.6 mSv[1][28]. Some of the main characteristics of the lunar as opposed to those of the earth's are summarized in Table 1.

	Moon	Earth
Equatorial radius	1737.5 km	6371 km
Mass ratio	1:81	1:1
Surface gravity	1.624 m/s^2	9.80665 m/s^2
Escape velocity	2.376 km/s	11.189 km/s
Atmospheric pressure	10^{-13}atm	1 atm

Table. 1. Some characteristics of the Earth the Moon [29]

1.3. Space solar cells

1.3.1. Space-specific conditions and requirements for solar cells

The qualification and quaility requirements for solar cells for potential space usage are naturally much higher and more specific than of those for the terrestrial application. Regardless of the mission type, the success of any space vessel greatly depends on the performance of the solar cells, therefore every single environmental detail and potential hazard should be considered while verifying the capability of a specimen to be utilized in space in a closely foreseeable manner, needless to mention that the possibility of repairing or replacing one during a mission is quite limited. As a rule, the characterization requirements for a solar cell is fully defined by the mission type, but there are a set of standards that are constant for each and every one of those.

- High efficiency to weight ratio, as the transportable cargo space is limited and transportation cost per unit mass and volume is quite high.

- High efficiency due to the highly limited are for the solar cells to be mounted on the vessel.

- Resistance to severe ionazing radiation present in space, especially in the Van Allen radiation belt – a zone near earth with intense presence of energetic charged particles. High-energy proton and electron irradiation will cause semiconductor materials to develop lattice defects, that for instance will act as recombination centers and deteriorate the output power of a solar cell. Anomalous behavior of the solar cell and electronics can also be the case due to the electrostatic charge accumulation and discharge caused by the interaction of the space vessel with environment packed with electrically charged particles.

- As solar arrays act as thermal collectos and accumulate waste heat, the cell temperatures must be kept as low as possible, as it is in direct correlation with the cell efficiency.

- Resistance to intense UV radiation.

- Resistance to corrosion in the lower earth orbit due to the formation of atomic oxygen (O – single atom of oxygen making up 96% of lower earth orbit).

These are the factors that have primarily determined the direction of evolution in the manufacturing and testing methods of space solar cells. Today the set of standard tests for different mission types is well defined to demonstrate the capability of a photovoltaic device to operate in space under different mission-specific conditions.

1.3.2. Evolution of Solar cell types

1.3.2.1. Silicon cells

Silicon solar cell was the pionner in the field of space photovoltaics. Since the year of 1954 Single-crystal, poly-crystal and amorphous Si space solar cells had been utilized the most for a couple of decades. Initially the paramaters of of these cells were quite low compared to contemporary standards. For instance, according to different sources the efficiency of Si cells used to be 7-10% for several years. Gradually, acquiring more information about specific behavior of a cell in space and sophisticationg the manufacturing process along the way the characteristics have been getting better decade by decade. For instance, initial cells contained a single-crystal N-type silicon and a P-type emitter, however later it was shown that the ones with P-type silicon and an N-type emitter are more radiation resistant, which caused the manufacturing to mostly shift from P/N cells (l N-type silicon and a P-type emitter) to these ones. Another notable advance was the invention, incorporation and improvement of back surface contact (BSF) in the 1960-70s which further propelled the cell efficiencies. A great leap in this parameter was especially fueled by the introduction of PERL structure - A cell with a passivated emitter due to the presence of strongly adhering oxide at the front surface to hinder surface recombination and a locally diffused rear at the metal contacts to minimise recombination there as well. By means of this technology alongside with HES-IBF (High efficiency silicon – integrated bypass function) efficiencies over 20% in space contidions were achieved. While this may not seem much compared with other material choices and the radiation resistance of a

silicon solar cell is not the best out there, it was still the way to go up to the 1990s. With the reasons being easier and much cheaper manufacturing processes, relatively light weigt of the cells, abundance and environmentaly friendliness of the material[1][30].

1.3.2.2. lll – V cells

Even though crystalline silicon was used predominantly for space solar cells, the rapid increase in the power requirement of the satellites called for a new solution with potentially higher conversion efficiency and more superior radiation resistance. For these reasons, since the early 1990s III - V cells have been favored over crystalline silicon. III – V cells had been the subject of research in the 1980s as well when GaAs and InP cell efficiencies reached 15-18%, however these approaches did not find practical implementation due to the reliability, predictability and consistency silicon cells had. These compound semiconductors are derived by combining group III elements, such as Al, Ga, In with group V elements, most importantly N, P, As and Sb. InP had demonstrated efficiencies over 18% alongside with excellent radiation tolerance, however except for missions with exceptionally high radiation levels the focus has mainly shifted towards GaAs solar cells. This can be explained by several disadvantages that InP possesses. Lattice mismatches of InP between Si and Ge as large as 8% and 4% respectively make it difficult to qualitatively grow it on these substrates, regardless to mention that InP is also a more expensive material[1], [6], [30], [31].

GaAs cells have demonstrated to be a great substitution to silicon ones due to high efficiency accompanied by high tolerance to degradation under space radiation – not something one would come across among silicon solar cells, meaning that efficiency of a GaAs cell would be considerably higher than that of a silicon cell for equivalent radiation tolerance. GaAs cells are also more resistant to degradation at high temperatures due to higher bandgap of 1.43eV as opposed to 1.11eV of silicon (300K)[31]. Last but not least, by means of MOCVD – Metalorganic chemical vapor deposition, also known as OMVPE – organometallic vapor-phase epitaxy, GaAs cells demonstrated capability to be produced in industry drove qualities initially on GaAs substrates[6].

Even though GaAs solar cells had proved superior to silicon ones, there was one more obstacle to overcome. Despite higher absorption coefficient and a direct band gap, this material which is around twice as dense as silicon (5.32 g/cm^3 versus 2.329 g/cm^3) still did

not allow for lightweight and efficient arrays, which is crucial for the space application. Higher efficiency should have made up for reduced area, however improvements had still to be made. Germanium was thereby adopted as a replacement for GaAs substrate. First of all it is less expensive, it also demonstrates pretty close lattice parameter and thermal expansion coefficient allowing for more reasonably priced, good crystal quality GaAs specimens, but most importantly Ge is mechanically stronger than conventional GaAs substrate, which gives possibility to make the cells thinner, thus reducing the weight parameter[31].

Consistent improvement to achieve higher efficiencies and better designs evolved conventional solar cells into dual junction ones grown on germanium substrates. These in turn, gave rise to multi – junction cells in the early 2000s. Offering efficiencies over 30%) and good resistance to radiation, $Ga_{0.5}In_{0.5}P/Ga_{0.99}In_{0.01}Ar/Ge$ structures have become the main solar energy generators for contemporary space missions. As the theoretical efficiency of multi-junction solar cells is much higher depending on the number of junctions and different fabricating methods, the research is underway to increase this parameter beyond already achieved 39.2%[32]. One of the approaches worth mentioning is the Lattice mismatched or metamorphic one, which has already shown to be the means for achieving the highest possible conversion efficiency. The idea implies broadening the range of bandgaps in the multi-junction solar cell by changing and utilizing different lattice constants to achieve more suitable band gap range for better power conversion[33].

1.3.2.3. Advanced solar cell technologies

Higher-efficiency solar cells for space application are under development and researches have been recently focusing on 4 main advanced cell structures:

- **Inverted metamorphic multi-junction (IMM)** – One of the most promising technologies currently under development, as already mentioned above, serves to capture as much energy from the solar spectrum as possible. In this case the cell is grown the opposite direction relative to the traditional multi-junction devices. The sub cells are grown monolithically on a GaAs substrate which is then removed. The lattice matched or minimally mismatched top cells GaInP and GaAs are grown first, followed by independently heavily lattice mismatched (Using two CGBs – Compositionally graded buffers) $Ga_{0.73}In_{0.27}As$ and $Ga_{0.27}In_{0.53}As$. There main peculiarities of this structural sequence are reverse order of growing the cell

layers, usage of semiconductor materials with mismatched crystal structures and implementation of compositionally graded layers. CGBs guarantee the utilization of every portion of solar spectrum by allowing for growth of different semiconductor materials with different crystal structures on top of another, thus creating metamorphic structure without hindering the cell efficiency. What's more, the removal of the substrate produces ultra-light, ultra-thin flexible and efficient cell which makes the procedure ideal for the space application. These have already demonstrated record efficiencies over 33%[34]–[37].

- **Dilute nitrides** – These are Highly Mismatched Alloys of group III – V, into which dilute concentrations of nitrogen have been introduced. It has been demonstrated that among these materials there is a very strong dependence of the band gap on the nitrogen content, which has made them a great subject of interest for high efficiency hybrid solar cells. Introducing a material that would provide a 1eV bandgap to absorb the infrared spectrum of solar radiation has been considered as one of the main possibilities to increase the multi-junction solar cell efficiencies. The latest material to do just that and in addition be a lattice-matched to other semiconductor materials used in multi-junction solar cells is GaInNAsSb, the band gap of which can be tune from 0.8eV to 1.4eV while maintaining the lattice-matched compound. Grown with the hybrid MBE-MOCVD method combining MOCVD (Metalorganic chemical vapor deposition for GaInP/GaAs cells) and MBE (Molecular beam epitaxy for dilute nitrides) 3 junction solar cells containing dilute nitrides, such as GaInP/GaAs/GaInNAsSb, have already demonstrated efficiencies over 31% at AM0 conditions. Having been scarcely implemented for only several years, these have demonstrated excellent radiation resistance with degradation factors surpassing those of conventional InGaP/InGaAs/Ge 3 junction solar cells. Currently under development are 4, 5 and 6 junction solar cells containing dilute nitrides that are expected to achieve efficiencies over 36%, with 4 junction ones by Solar Junction Corp. having already demonstrated 33% under AM0 conditions[38], [39].

- **Semiconductor wafer boning technologies (SBT) –** One of the most powerful technologies in development today combining lattice-mismatched materials without any dislocations created. Wafer bonding process allows for the

integration of non-lattice-matched semiconductors by isolating the associated misfit defects to the bonded interfaces[40].

- **IN-SITU resources –** Development and direct fabrication of photovoltaic cells in the extraterrestrial environment from indigenous resources. The feasibility of manufacturing solar cells on the surface of the moon has been considered a great opportunity since the beginning of the 1990s. In the case of the lunar soil, the abundance of silicon and presence of other usable materials in the form of oxides among rock forming minerals (Ilmenite – $FeTiO_3$, Anorthite – $CaAl_2Si_2O_8$ and pyroxene – $(Ca, Mg, Fe)SiO_3$) makes lunar production of silicon and amorphous silicon solar cells possible[41].

1.3.3. Quality requirements and standards for space solar cell usage and transportation

From the moment of take-off to the varieties of harsh environment present in different regions of space, a solar array is subject to extraterrestrial interactions that degrade not only the PV device components, but also the substrate materials and circuitry. Therefore, for a photovoltaic array to operate in a safe, stable and predictable manner, it is crucial to assess every element of the demanding environments. The minimal requirements for every device include the key elements that are true for almost every mission regardless of mission-specific details. These are: Radiation by short-wavelength ultraviolet and long-wavelength infrared portions of solar spectrum that photo-ionize and heat materials; Plasma environments that influence electrostatic charging of material surfaces; Thermal cycling inducing thermal expansion and contraction of the array components; High energy electron radiation that greatly reduces the output power of III – V type cells; Regardless to mention the severe mechanical stresses during take-off. These are the minimal, general complexities of cell working environment that need to be accounted for through realistic testing. However, even these do not cover all the peculiarities of a very wide range of missions. For instance, the solar-powered outer planetary mission require that the cells operate in extremely low solar irradiance and low temperature environments, long-life capability and high reliability for obvious reasons. While the inner planetary missions would call for a much wider range of capabilities depending on whether the mission is orbital, surface or areal. The typical implications would be high solar flux; high temperatures; corrosive environment resistance;

Certain testing protocols have been developed and standardized to assess the performance of solar cells and photovoltaic arrays in such conditions[4], [42]

1.3.3.1. Qualification tests

The standard for Qualification and Quality Requirements for Space Solar Cells establishes qualification, characterization, and quality requirements for all solar cells intended for operations in space. The paper defines standard tests, environmental conditions, procedures, and systematic methods for verifying the capability of a photovoltaic cell device to operate in the environment in space. Of these, relevant ones to the context of this thesis are listed below. Nevertheless, not all the tests were able to be performed in TTÜ labs, performed tests with explanations are in Section 2 – Methods and Results.

- **Characterization tests**[42]
    - Electron radiation effects
        - Electrical test
        - Electron radiation exposure
        - Electrical test after radiation
        - Reverse bias exposure
        - Electrical test after reverse bias
    - Proton radiation effects
        - Electrical test
        - Proton radiation exposure
        - Electrical test after radiation
        - Dark reverse bias exposure
        - Electrical test after reverse bias
    - Bend test
    - Breaking load determination
    - Light I-V characterization for multiple temperatures
    - Quantum efficiency
    - Dark I-V characterization

- Capacitance effects
- Solar cell electrostatic discharge sensitivity test
- Accelerated life test

1.4. Solar cell characterization techniques – Current-voltage characteristics

The current-voltage characteristics of a solar cell allows for a graphical representation of the performance of a cell by demonstrating the relationship between the current and voltage at particular values of irradiance and temperature (Fig. 2.).

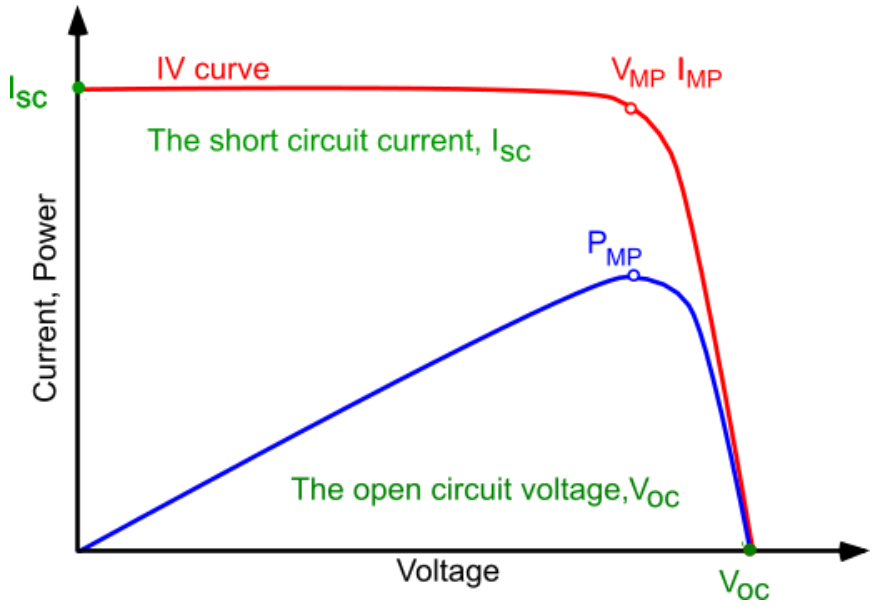

Fig. 2. Current-voltage characteristics of a solar cell under dark and illuminated conditions[43]**.**

The curve demonstrates the diode characteristics of a solar cell and summarizes its following fundamental electrical properties that precisely describe its performance. Characteristics of a p – n junction solar cell under steady illumination can be described using the model as[44]:

$$J = -J_{ph} + J_0\left(e^{\frac{qV}{nKT}} - 1\right) \quad (1)$$

- **Short circuit current I_{sc} and current density (j_{sc})** – Greatest value of the current generated by a cell in the short circuit conditions, i.e., $V = 0$.

$$J_{sc} = q\int_{hv=E_g}^{\infty} \frac{dN_{ph}}{dhv}\, d(hv) \quad (2)$$

J_{ph} – photogenerated current density; V – terminal voltage; k – Boltzmann constant; n – ideality factor; J_0 – temperature dependence of reverse saturation current density; N_{ph} – initial photon flux, v- frequency of light.

- **Open circuit voltage (V_{oc})** – The maximum value of voltage provided by the cell when it is not connected to an external load, i.e., in an open circuit condition.

$$V_{oc} = \frac{kT}{q} \ln\left(\frac{J_{sc}}{J_0} + 1\right) \quad (3)$$

- **Fill factor (FF)** – Describes the shape of the illuminated current-voltage curve. It can be considered the defining term for the overall performance of the cell ultimately demonstrating the quality of a device. Fill factor is expressed with the equation:

$$FF = \frac{Vmpjmp}{Vocjsc} \quad (4)$$

where V_{mp} and j_{mp} represent the photovoltage and photocurrent density at the maximum power point, respectively. V_{oc} is the open circuit voltage and j_{sc} is the short circuit current.

The fill factor is directly related to the values of the cell's series and shunt resistances. Namely, greater shunt resistance, greater the external photocurrent, thus higher the fill factor. In turn, increasing the series resistance leads to the efficiency of the charge collection, thereby lowering the fill factor.

- **Conversion efficiency (η)** – Ultimate characteristic of a photovoltaic cell expressing the ratio of the maximum power output extractable from the device to the incoming power.

$$\eta = \frac{V_{mp} j_{mp}}{P_{in}} \quad (5)$$

where V_{mp} and j_{mp} represent the photovoltage and photocurrent density at the maximum power point. P_{in} is the value of the incoming irradiation power.

1.5. Monograin layer solar cells and crystalsol's monograin based PV technology

The concept of using powder technologies to produce solar cells dates to the 20th century. Several patents were filed concerning the production of photovoltaic devices from silicon powders; multipurpose use of monograin membrane modules; Development of Spherical Solar Cell technology which is comprised of an array of single-crystalline silicon spheres with each one of these functioning as an individual solar cell.

Monograin is a single-crystalline powder particle consisting of one single crystal or several single-crystalline blocks grown into a compact grain. Consisting of a thick layer of grains embedded into an organic resin. Powder technologies eliminate many shortcomings that relatively developed fields of photovoltaics demonstrate. Particularly, powder technologies are the cheapest and simplest in production; possess the single-crystalline structure of every single grain; offer the possibility for large surface area, good reproducibility with maximum use of materials and the possibility of making flexible devices ultimately combining the attractive photoelectric parameters of monocrystals and respective advantages of polycrystals[45], [46].

Monograin layer solar cell technology is currently developed by crystalsol gmbh, where flexible photovoltaic modules offering considerable advantages due to the simplicity and low-cost production of the process. Therefore, apart from the fact that CZTS is highly potent and promising material for space photovoltaics on its own, simple, lightweight and easily transportable production line adds greatly to the value. Company's patented technology includes two separate stages – the production of light absorbing semiconductor material and the production of the PV-membrane. Ultimately, the pinnacle of crystalsol's technology is the unique simplicity of upscaling to larger areas eliminating traditional, time consuming and costly processes, thereby allowing for the integration in architecture, portable lightweight modules, automotive industry and other applications.

The production of CZTS powder takes place in Tallinn, Estonia. The process of powder production can be described as follows[24], [47], [48]:

- Monograins with diameters as much as 25 µm are grown from elemental (Copper, zinc, tin, sulfur and selenium) or binary (Cu_2Se, ZnSe and SnSe) precursors, which are mixed with a flux material (inert salt) and heated in either evacuated quartz ampoules or graphite containers in inert atmosphere (Depending on the amount) to temperatures above the melting point of the flux material.

- The growth of the powder grains is facilitated with the salt acting as a solvent for the metal ions.
- After cooling the salt mass is dissolved in water and the CZTS powder is separated via sieving, (Fig.3. a).
- Too fine grains are reproduced, too big ones are milled.
- The surface is cleaned by washing and etching followed by annealing.
- Approximately 30nm thick CdS layer is deposited around the crystal by chemical bath deposition to protect the surface and at the same time provide the n-type buffer layer to form the junction.
- Very stable, easily storable and transportable monograins are obtained (Fig.3. b).

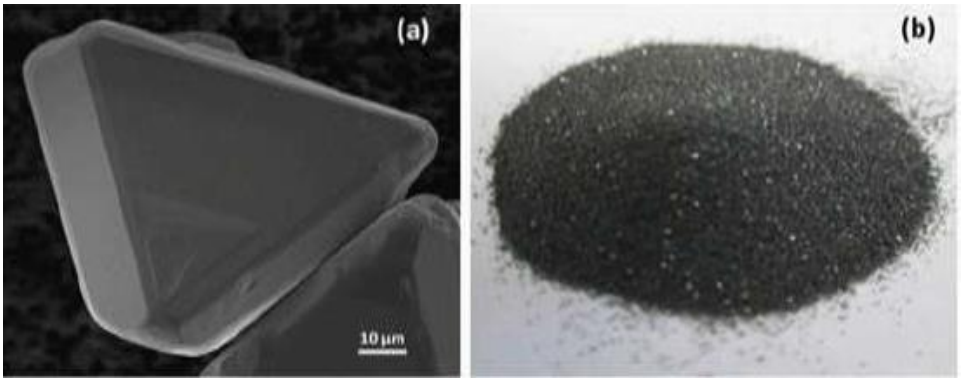

Fig. 3. SEM image of a CZTS single crystalline grain (a) and CZTS monograin powder[47].

The innovative module production process uses a simple, low-cost printable roll-to-roll technology allowing for a very high output and yield typical for the printing industry. The production process runs as follows[24]:

- Coating the substrate (PET foil) with the polymer so that the polymer maintains portion of its liquidity and viscosity.
- Embedding serial connection wires.
- Partially embedding the grains into the insulating polymer matrix in a way that a portion of each grain remains above the layer.
- Covering the protruding parts of the grains with the transparent front contact (as a rule ZnO/AZO) followed by a transparent and highly conductive silver nanowire in order to reduce the sheet resistance of the TFC.
- Mechanically stabilizing and protecting the front side.
- Abrasing the solidified polymer on the other side of the membrane to expose the grains and remove the CdS buffer.
- Printing the back contact.

The graphical representation of the entire process can be seen in the Figure 4 below.

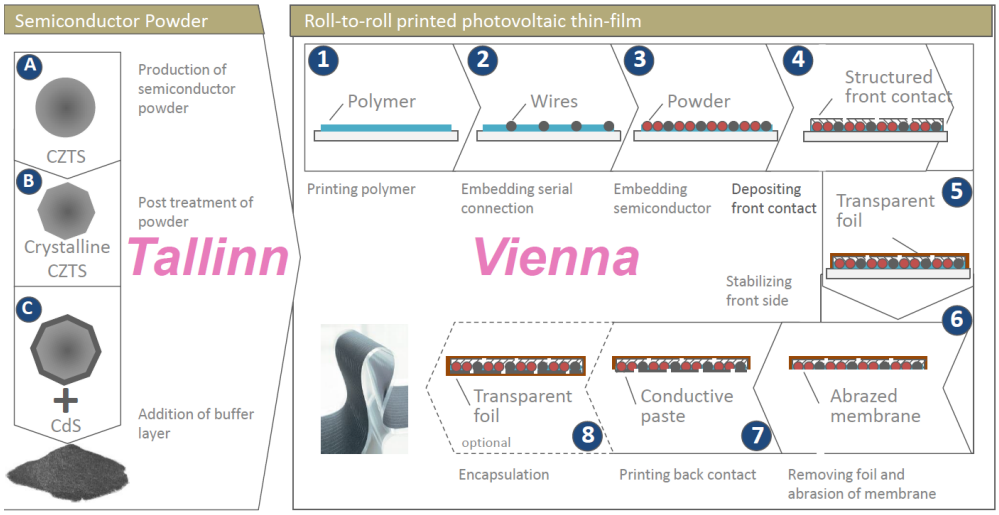

Fig. 4. Section of crystalsol's monograin layer solar cell[47].

The design, production and example of the photovoltaic cells can be seen in the figures below.

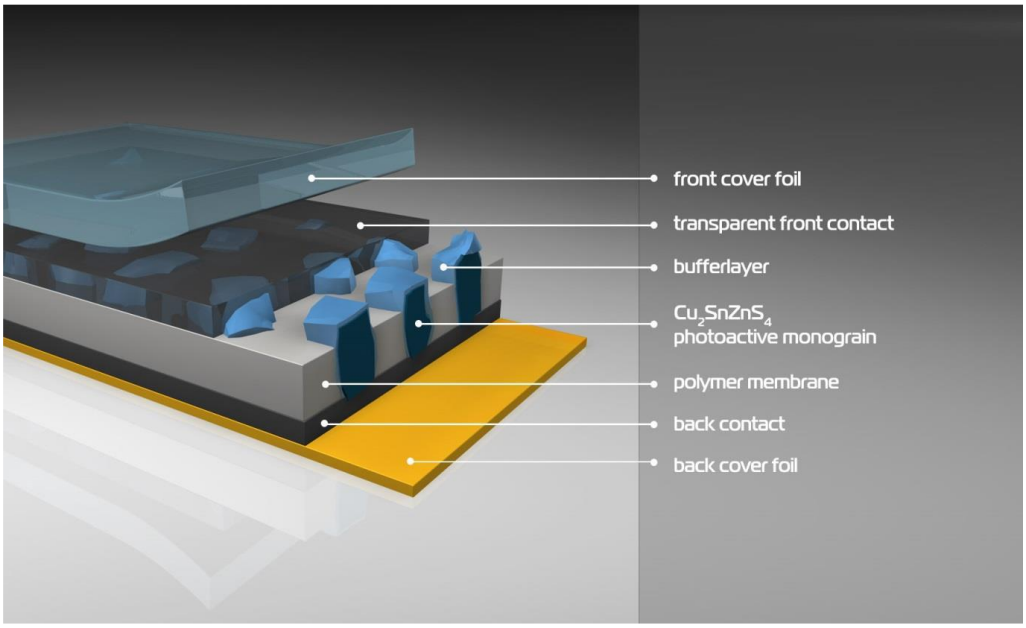

Fig. 5. Section of crystalsol's monograin layer solar cell[47].

Fig. 6. Flexible solar cell[24].

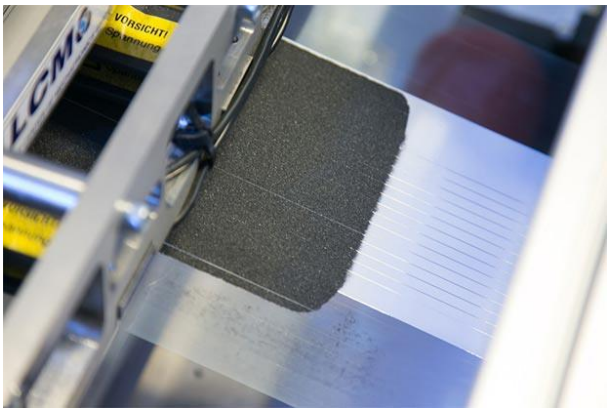

Fig. 7. Production line of crystalsol solar cells[49].

2. Methods and Results

Within this project, crystalsol's CZTSSe solar cell samples have been analyzed, investigated and experimented with to assess the performance and the degradation mechanisms of the devices in space conditions simulated in the laboratories of Taltech. All twelve tested solar cell samples were fabricated from the same absorber material and assembled according to standard crystalsol technology. Nevertheless, slight variation in the parameters was observed and taken into consideration.

The experimental procedure was adjusted to two circumstances – the range of available laboratory equipment and the specifications of the samples provided by the company. Particularly with the latter, the glass substrate present in case of all the samples played a major role in either choosing the possible experiment or adjusting one.

Having assessed the limitations mentioned the limitations above the experimental procedure was planned and respectively carried out as follows:

- **Vacuum stability tests**
- **Low temperature tests in the presence of vacuum**
- **Intense UV radiation tests**
- **High temperature tests**
- **Thermal cycling tests**

The performance of the solar cells before and after the experimental procedures is evaluated with I-V measurements performed with a Keithley 2400 Source Meter, Keithley Instruments Inc., Clevelend, Ohio, USA, with a 2 -wire measurement setup. The illumination is simulated by Newport Oriel AAA-class sun simulator, Newport Corporation, Stratford, CT, USA or halogen lamp. Critical electrical parameters - fill factor (FF), open circuit voltage (V_{oc}), short circuit current (I_{sc}) and efficiency (η) are measured and analyzed.

As additional means of analysis, scanning electron microscopy is utilized via Zeiss ULTRA 55, Carl Zeiss Microscopy GmbH, Jena, Germany instrument[50].

2.1. Vacuum stability tests

To make sure the samples are ready for the low temperature gradient tests which were to be conducted in the presence of high vacuum, the experimental process started with high vacuum tests alone. Integrity issues like encapsulation problems, presence of humidity and insufficient sealing could have crucial consequences for the performance of the cell in the vacuum environment.

2.1.1. Experimental procedure and results

The photovoltaic devices were placed in a vacuum chamber powered by Pfeiffer HiCube 80 pumping station providing vacuum level of 10^{-6} hPa. Keithley 2400 multimeter with a 2 – wired setup was used to measure the electrical characteristics under 100 mW /cm2 halogen lamp to be afterwards compared with those retrieved under standard test conditions. The aim of the process was to test and observe the mechanical and electrical integrity of the cells and analyze the changes, if any. The graphical representation of the standard versus vacuum environment behavior of the solar cells can be seen in the figures below. Five solar cell samples were subject to same experimental procedure to obtain broader image. A clear, well-defined and persistent behavior was demonstrated by all the devices, two of which are represented below.

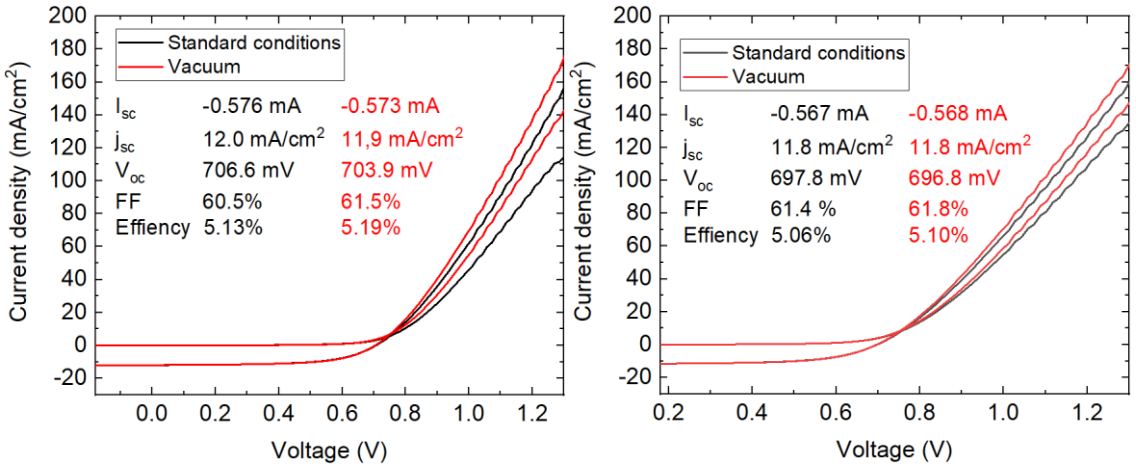

Fig. 8. J - V curves and electrical characteristics of two samples – Under standard test conditions and vacuum.

The obtained results demonstrated that the cells performed well in the high vacuum environment, even showing minute improvements in fill factor and efficiency values. Visual inspection did not reveal any apparent defects as well, practically excluding any kind of integrity, encapsulation or electrical flaws in the vacuum.

2.2. Temperature tests

The investigation of the dependence of the solar cell behavior on the temperature is extremely important, as in the terrestrial and more so in the extraterrestrial applications, the devices are subject to a very wide range of temperature gradients. In current thesis, two extremes and the transitions between these are simulated and studied.

The effect of the temperature on the open-circuit voltage, short circuit current, fill factor and the efficiency of the cell is governed by its diode characteristics, which are reverse saturation current density, ideality factor, series resistance and shunt resistance. The main temperature dependence of solar cells is generally governed by the temperature induced changes of the open-circuit voltage of the cell, which, in turn, is directly related to the ratio between the recombination rate of the carriers and the photogeneration rate in the cell. Carrier recombination in the neutral regions of the junction results in the leakage of the minority carriers across it in reverse bias. Therefore, reverse saturation current density, which is the measure of this leakage is a critical parameter as far as temperature dependence is concerned[44], [51].

It has been demonstrated by the studies earlier that the performance of the photovoltaic cells tends to degrade with the increase in temperature mainly due to increased carrier recombination rates. It has been shown that V_{oc} decreases and J_{sc} increases slightly with increasing temperature. Exponential increase of the reverse saturation current, thereby responsible for the rapid decrease of $V_{OC,}$ is also the case. Hence, fill factor and efficiency both decrease as well with the increase of the temperature. The formulation behind these phenomena is given below[44].

Temperature dependence of the band gap in the semiconductors given by Varshni equation:

$$\boldsymbol{E_g(T) = E_g(0) - \frac{\alpha T^2}{(T + \beta)}} \qquad (6)$$

$E_g(T)$ – Band gap at a certain temperature;

$E_g(0)$ – Bandgap value at T ≈ 0;

$\alpha \; and \; \beta$ – Constants for semiconductor materials

Short circuit current density is given by the equation:

$$\boldsymbol{J_{sc} = q \int_{hv = E_g}^{\infty} \frac{dN_{ph}}{dhv} d(hv)} \qquad (7)$$

N_{ph} – Initial photon flux

v - light frequency

According to this formula, the values of J_{sc} can be calculated for different temperatures by integrating the solar spectrum to the particular value of E_g acquired from (6).

From (3) the temperature dependence of open circuit voltage can be expressed as:

$$\frac{dV_{oc}}{dT} = \left(\frac{V_{oc}}{T}\right) + \frac{kT}{q}\left(\frac{1}{J_{sc}}\frac{dJ_{sc}}{dT} - \frac{1}{J_0}\frac{dJ_0}{dT}\right) \quad (8)$$

Efficiency can then be calculated at each temperature using the obtained corresponding values of V_{oc}, J_{sc} and FF at each temperature as follows:

$$\eta = \frac{V_{oc}J_{sc}}{P_{in}} \quad (9)$$

P_{in} – Intencity of the incident radiation

The changes in the band gap of a semiconductor material, in this particular case caused by temperature gradient, can be considered as and translated into the energy of the electrons in the material, in other words the energy needed to break the bond and create the electron hole pairs. The *cut-off* wavelength of photons with energy useful for the carrier generation depends on the band gap of the material and is given by the formula[44], [51]:

$$\lambda_g = \frac{hc}{E_g(eV)} = \frac{1240}{E_g(eV)} \quad (10)$$

h **–** Planck constant

c **–** Speed of light

2.2.1. Low temperature tests - Experimental procedure and results to date

A closed-cycle helium cryostat (Janis CCS-150) was utilized to study the temperature dependence of the cells on the temperature gradient from 320K to 20K. The samples were placed in a vacuum chamber at 295K, which was set to initially heat up to 320K and gradually drop to 20K with a step of 10 afterwards using Lakeshore temperature controller. Electrical characteristics were measured at every point. The trend of temperature induced changes of short circuit current, open circuit voltage, fill factor and conversion efficiency can be observed in the graphs below. Five solar cell samples were subject to same experimental procedure to obtain broader image. A clear, well-defined and persistent behavior was demonstrated by all the devices, two of which are represented below.

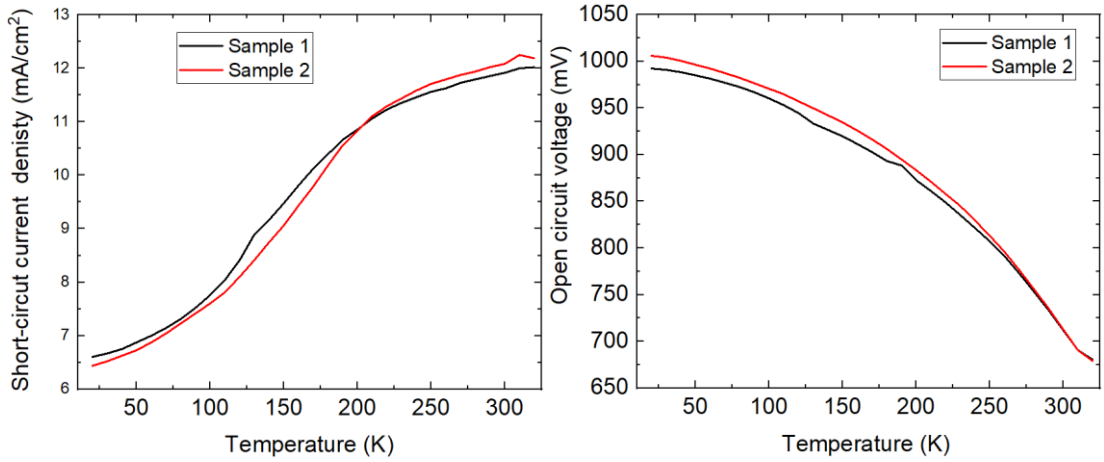

Fig. 9. Temperature induced changes of short circuit current density (left) and open circuit voltage (right).

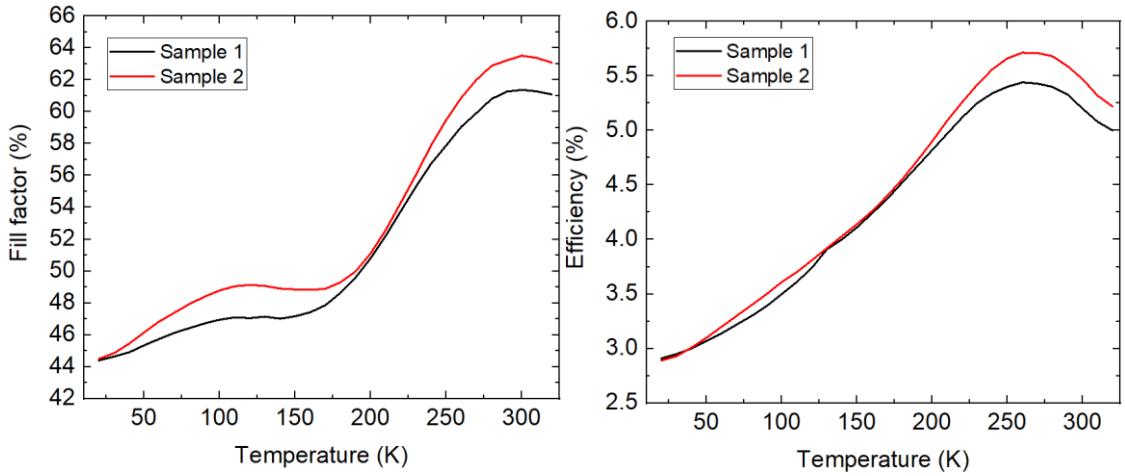

Fig. 10. Temperature induced changes of fill factor (left) and efficiency (right).

The samples demonstrate a clear, consistent behavior over the extent of the temperature gradient with a well-observable trend in the fluctuation of the electrical parameters. As expected according to the theoretical formulation in the previous chapter, short circuit current is measured to have constant, gradual decrease while the open circuit voltage value is increasing considerably with dropping temperature. The efficiency is measured for its highest values at 260K, while the fill factor is observed at its highest at 300K.

Moreover, as the experimental procedure was intended for a particular framework of lunar environment, three most relevant temperature points were analyzed in terms of IV curves as well. These, along with the respective electrical characteristics at temperature points of 290K, 90K and 20K can be seen in the figures below:

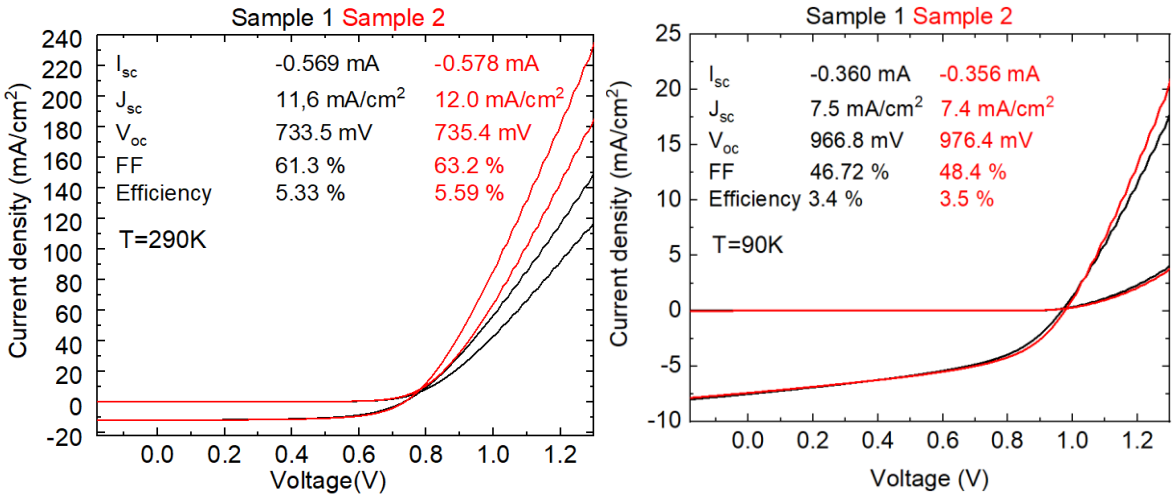

Fig. 11. J - V curves and electrical characteristics of two samples at 290K and 90K in vacuum.

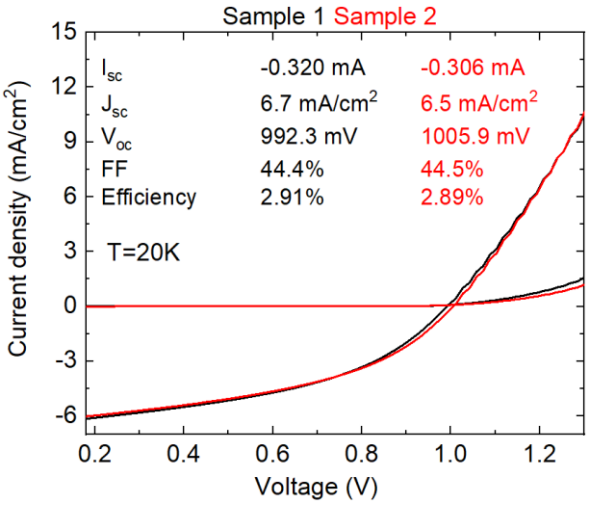

Fig. 12. J - V curves and electrical characteristics of two samples at 20K in vacuum.

It can be deduced that devices maintain a current-voltage characteristic curve typical to a solar cell with a gradual degradation of the electrical characteristics with the dropping temperature - in a consistent manner with the theoretical analysis and trends in figures 8 and 9.

As the samples underwent a wide temperature gradient from 320K to 20k and back, it was sensible to check their performance and visually inspect before proceeding with the experimental procedure. Electrical measurement showed no signs of any changes in the performance of the cells, indicating that the monograin layer solar cells are able to effectively operate at extremely low temperatures as well.

2.2.2. High temperature tests

To simulate the high temperature exposure on the lunar surface, two independent, similar samples were placed in a 125°C furnace. The table and the graphs shown below represent the numerical changes of electrical characteristics of two samples placed in the furnace for an hour and for two hours (Sample 1 and Sample 2 respectively).

	Initial		**After treatment**	
	Sample 1	Sample 2	Sample 1 (1h)	Sample 2 (2h)
Short circuit current density (mA/cm^2)	17	16.8	17.3	17.1
Open circuit voltage (mV)	706	695	684	669
Fill factor (%)	59	58	55	51
Efficiency (%)	6.9	6.6	6.5	5.9

Table. 2. High temperature induced changes of electrical parameters of two samples.

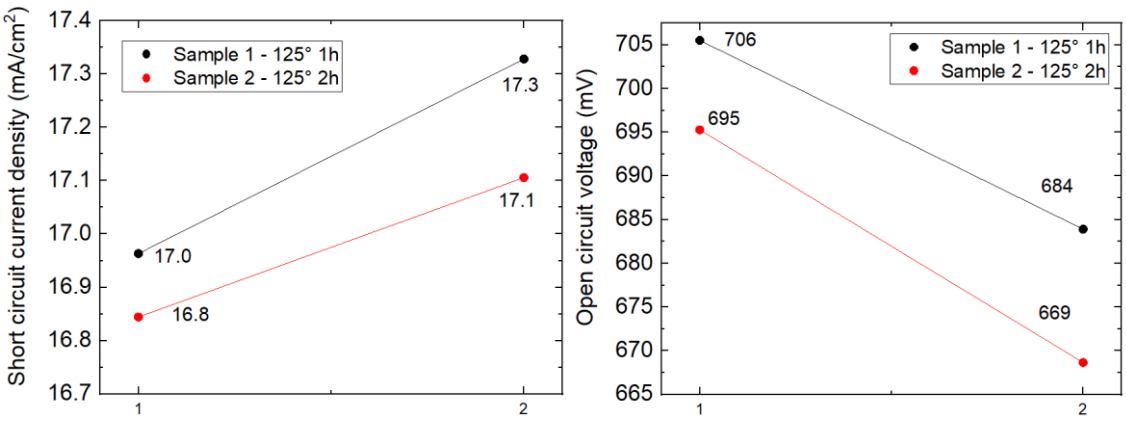

Fig. 13. High temperature induced changes of short circuit current density (left) and open circuit voltage (right); 1 – Initial value; 2 – After treatment.

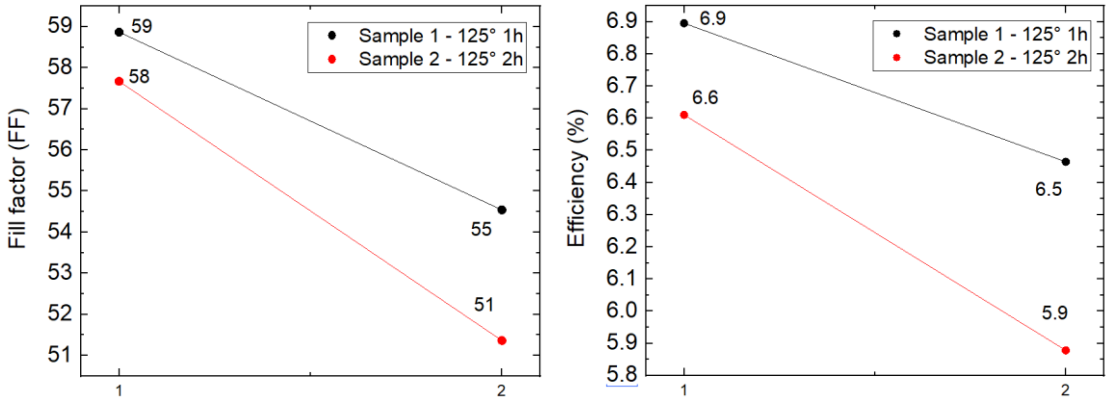

Fig. 14. High temperature induced changes of fill factor (left) and efficiency (right); 1 – Initial value; 2 – After treatment.

As expected, most of the parameters demonstrated considerable degradation after the high temperature treatment, except J_{sc}, which slightly increased, most likely explained by the reduction of the interface recombination. An additional, independent sample was further placed in the furnace for the duration of twenty hours to observe the extent of the damage to the mechanical integrity of the photovoltaic cell after an extended period. Visual inspection showed no signs of visible damage to the integrity of the device, however the electrical characteristics demonstrated further degradation. Graphite back contacts were assumed to be one of the mechanisms of such rapid deterioration of the cell's performance. These were manually replaced with new ones, as a result of which an average improvement of 15% was measured in the efficiency of the cells.

To contemplate the mechanical stability of the cell after the high temperature tests, scanning electron microscopy was used. The following graphics represent the comparison of a new cell

with the one after a twenty hour 125°C treatment. Like the visual inspection, SEM images showed no visible signs of mechanical damage as well.

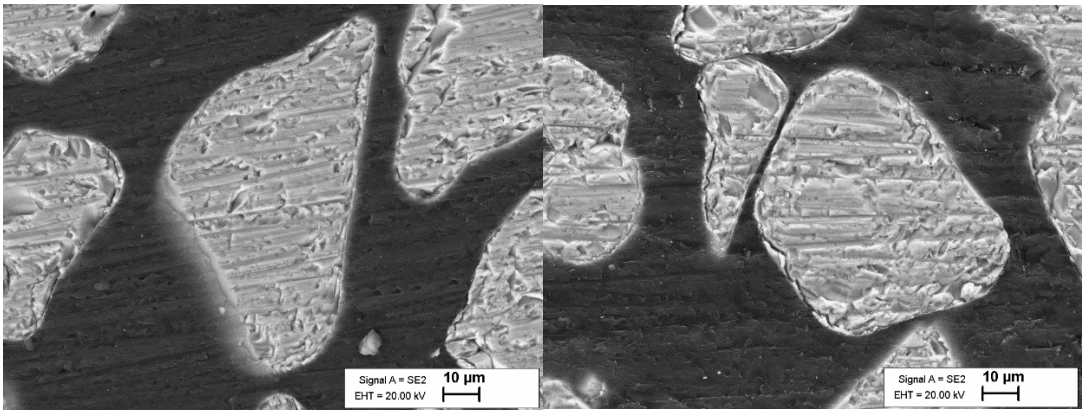

Fig. 15. SEM images of new (left) and tested (right) solar cells.

2.3. Radiation tests

Since the radiation in the space environment is severe, solar cells are required to possess enough radiation-resistant characteristics. To operate a photovoltaic array in space it is essential that thorough testing be done to account for every aspect of the extraterrestrial environment. As far as possibilities for radiation induced degradation is concerned, key considerations are high energy electron radiation, high energy proton radiation and solar photon radiation.

High energy proton and electron irradiation is known to induce atomic displacements, lattice defects in the semiconductor materials, thereby generating vacancies, interstitials and different types of complex defects (vacancy-impurity pair, interstitial-impurity pair, di-vacancy). These, in turn, act as recombination or carrier trapping centers that result in significant decrease in the performance of the device[30]. According to[52] lll – V type photovoltaic cells have demonstrated to be very sensitive to charged particle radiation. For example, in case of GaAs, minority carrier lifetime is the major radiation-sensitive parameter, caused by the displacements induced by the radiation and the disruption of the periodic lattice structure[53].

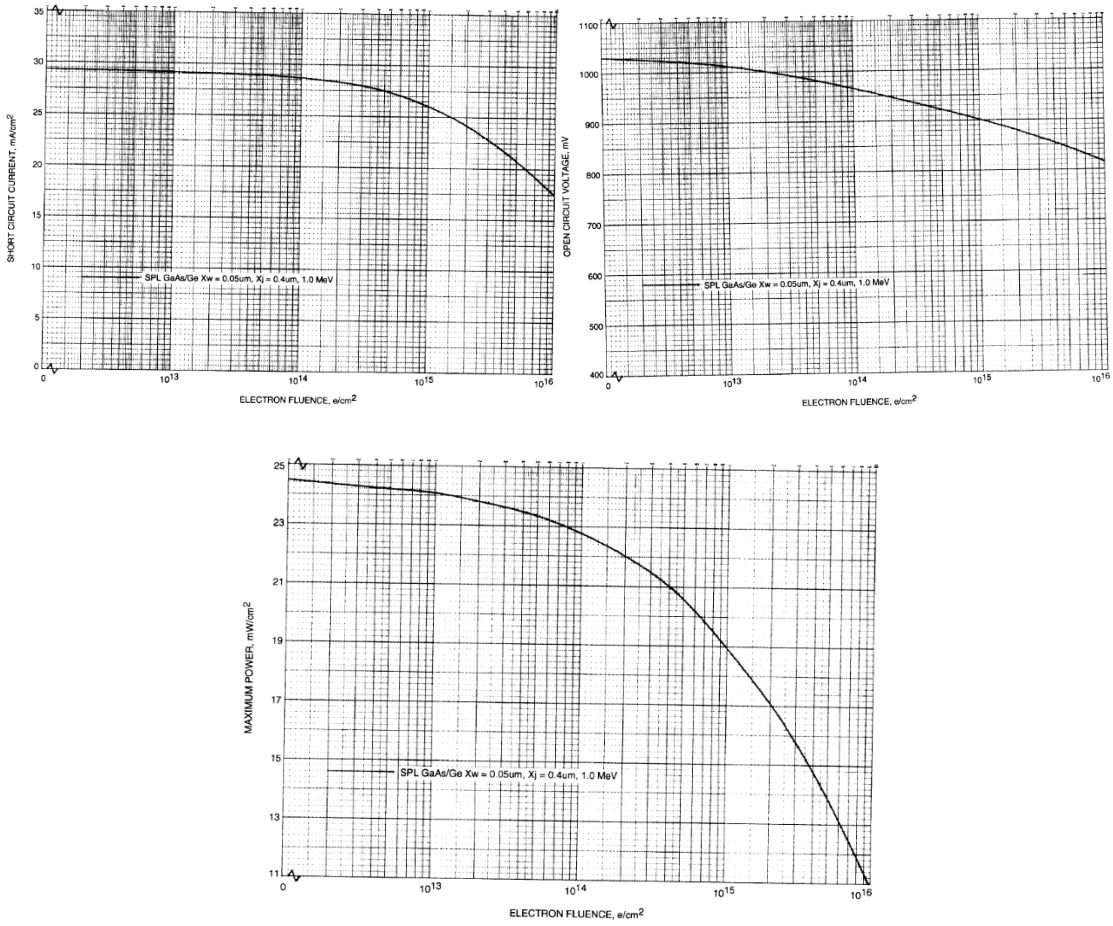

Fig. 16. I_{sc}, V_{oc} and P_{max} vs. 1 MeV Electron Fluence for Spectrolab GaAs/Ge solar cells[53].

Solar photon radiation, which is the essence of the operation of a photovoltaic device, is known to be hazardous as well. Namely, the short wavelength ultraviolet and long-wavelength infrared portions of the spectrum photo-ionize and heat the materials respectively[52]. In the case of conventionally used types of crystalline silicon solar cells, light induced degradation a very well-known phenomenon resulting in the decrease of the output efficiency of the device shortly after the first exposure to light[54]. Even though well observed over the last decades, this multifaceted problem in silicon solar cells has not been specifically identified and explained yet, in terms of precise causing mechanisms and responsible defects. However, it is recognized that boron-doped crystalline silicone solar cells manufactured on Czochralski wafers demonstrate light induced degradation generally associated with boron-oxygen defects in the wafer followed by a reduction in the minority-carrier lifetime in the bulk. Light induced degradation is a major disadvantage of amorphous silicon thin films as well. Due to the Staebler-Wronski effect[55]. the efficiency is reduced due to the destruction of weak silicon-hydrogen bonds in the absorbing layer, resulting in increase of the density of the defects[56], [57] .

Ultraviolet radiation induced degradation, therefore, is nonetheless interesting and important for the extraterrestrial applications of the cells given the fact that the intensity of UV in space is much higher than on the earth. According to the literature, extensive studies have been published concerning the UV exposure degradation of different, commercial c-Si photovoltaic modules. The literature review from NREL PV Module Reliability Workshop thoroughly discusses the research on the factors affecting the degradation and eventual failure of solar modules due to prolonged UV exposure[58]. Decrease in the performance and losses due to EVA (Ethylene-vinyl acetate) encapsulant browning and intrinsic crystalline silicon degradation is discussed[59]. A report from 2005 demonstrates an interesting trend – linear relationship between short circuit current degradation rates and the ultraviolet radiation dose[60].

Sample	Rate (%/GJ/m^2)	r^2
Cast-Si TiO_2 AR #1	+0.15	0.024
Cast-Si TiO_2 AR #2	-0.51	0.173
Cz-Si TiO_2 AR #1	-2.41	0.908
Cz-Si TiO_2 AR #2	-2.70	0.906
Cz-Si no AR #1	-0.98	0.532
Cz-Si no AR #2	-1.38	0.605

Fig. 17. I_{sc} degradation rates and linear-fit correlation coefficients for the samples encapsulated with EVA in module-style packages under Solatex superstrates[60].

The report concludes and points out that the degradation rates vary with the cell types Authors bring out and compare the results from unencapsulated, the Solatex/EVA encapsulated and UV-blocking modules, graphical representations of which can be seen in the plots from the report below.

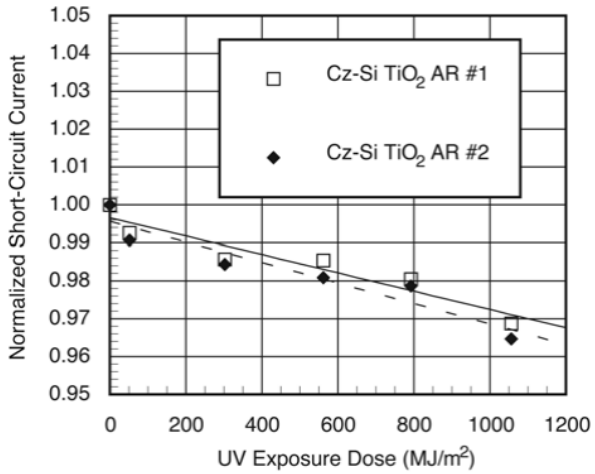

Fig. 18. Normalized I_{sc} versus total UV exposure dose for Cz-Si samples with TiO_2 AR coating and encapsulated with EVA in module-style packages under Solatex superstrates[60].

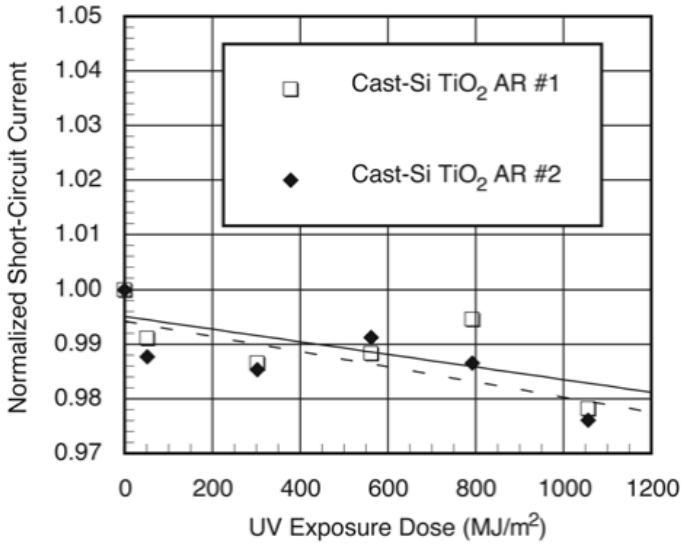

Fig. 19. Normalized I_{sc} versus total UV exposure dose for unencapsulated cast-Si samples[60].

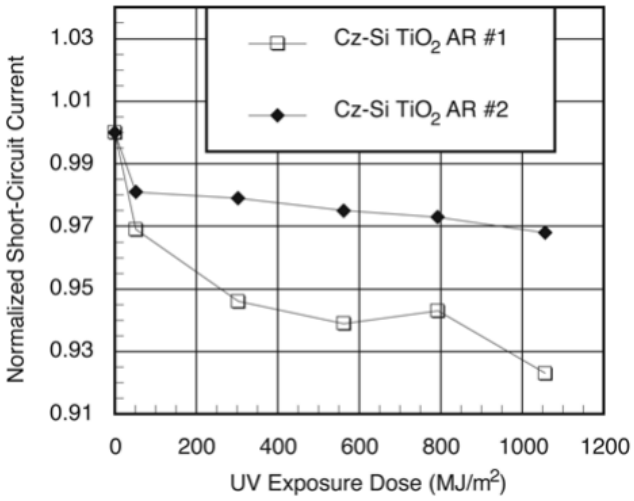

Fig. 20. Normalized I_{sc} versus total UV exposure dose for Cz-Si samples with encapsulated under UV-blocking substrates with EVA[60].

Similar studies have been conducted to study the effects of UV on power degradation of multi-crystalline silicon[54], inverted organic[61] and perovskite solar cells[62].

2.3.1. Experimental procedure and results to date

To evaluate the effect of intense UV light to the solar cells, three samples of crystalsol's production have been analyzed and subject to the ultraviolet light illumination. Themier TH 2108 N mercury lamp with irradiation of 38 mW/cm^2, the spectrum of which can be seen in Figure 20, was used during the experiment. Among the samples, one sample had already been subject to low temperature (320 – 20 K) gradients and the other two with no prior tests at all. The samples were placed in the radiation environment for consecutive duration of 5 and 12 minutes and measured before and after every cycle for short circuit current, open circuit voltage, fill factor and efficiency values. Respective IV curves were retrieved as well.

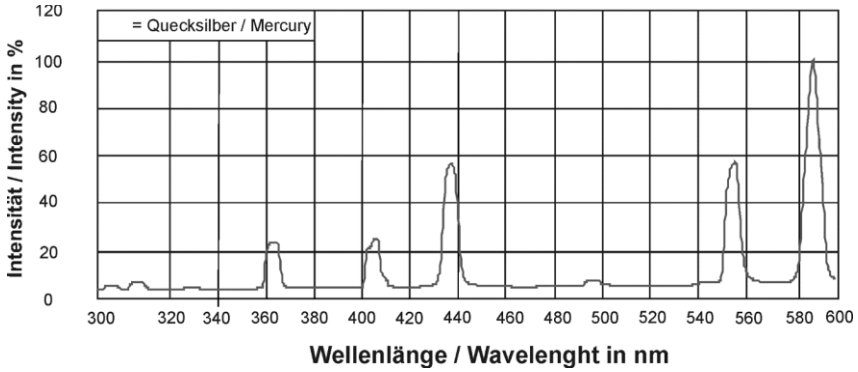

Fig. 21. Spectrum of the Themier TH 2108 N mercury lamp.

The results for the CZTSSe monograin solar cells did not quite follow the commonly observed trends from the literature, as in the case of crystalline silicon for example. Instead, interestingly, all the measurements taken (3 samples per 4 contacts each) demonstrated increase in the output parameters after the first, five-minute exposure to the ultraviolet radiation environment, as it can be seen on the Figures 21 - 24. Similar behavior has also been noticed with a CIGS solar cell – Yu et.al [63]explain similar phenomenon, whereby slight increase of solar cell parameters is observed after UV exposure especially in series and shunt resistance, by neutralizing deep acceptor defects in the absorber near the interface. It is important to note, however, that this phenomenon was unique to the very first shorter exposure – the consecutive measurements after following, longer exposures revealed the expected degradation trend of the cells with the increasing dose of radiation. Additionally, browning of the polymer was observed, which could partially be responsible for the degradation of performance. The changes of the cell parameters over the course of the experimental procedure can be seen in the figures below. The experimental procedure included three samples – one used during the low temperature tests and two fresh ones. Points 1, 2 and 3 on the x - axis of the graphs represent the initial values, those after 5-minute UV exposure and after 12-minute UV exposure respectively.

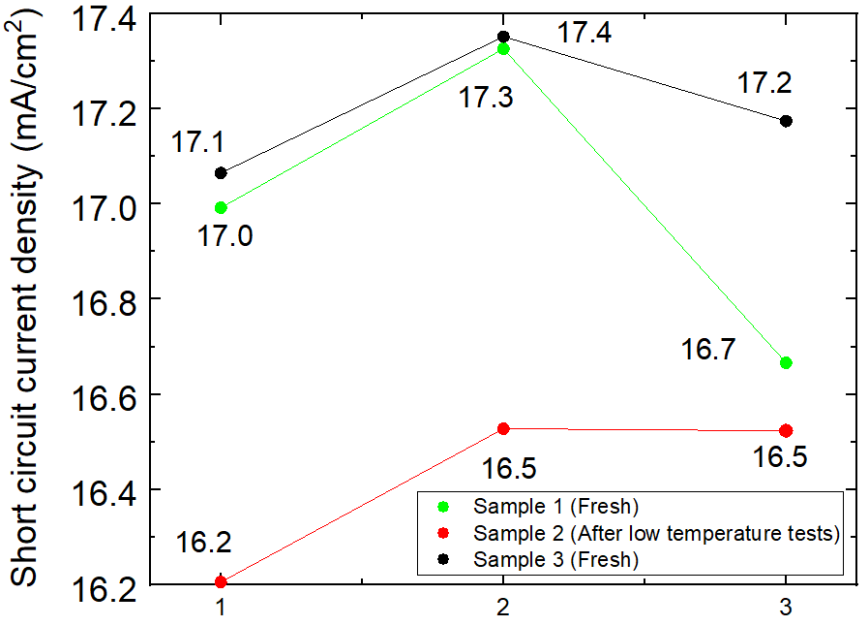

Fig. 22. Changes of short circuit current density of three crystalsol CZTS cells after UV exposure for five and twelve minutes. 1 – Initial; 2 – five-minute exposure; 3 – twelve-minute exposure.

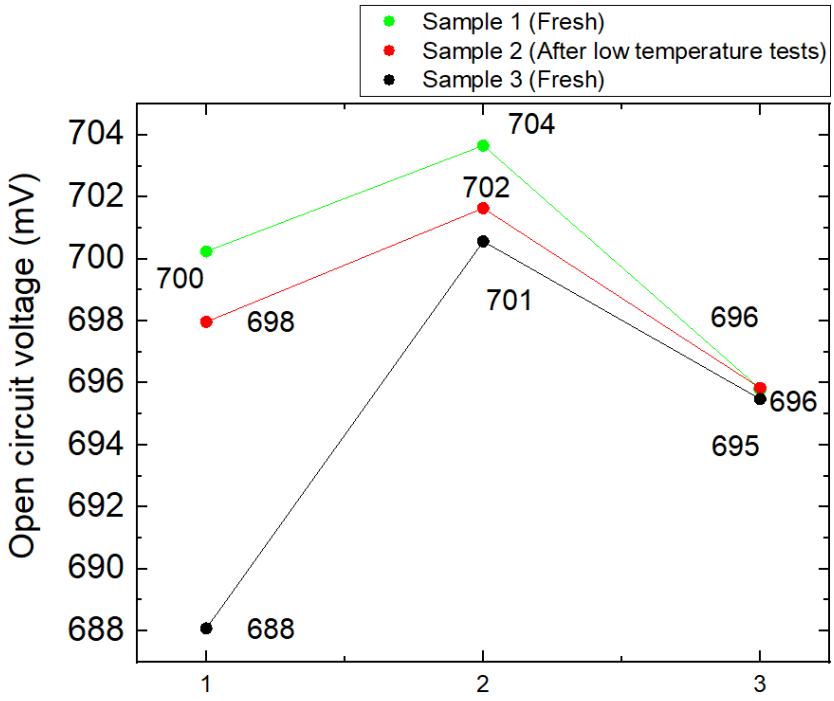

Fig. 23. Changes of open circuit voltage of three crystalsol CZTS cells after UV exposure; 1 – Initial; 2 – five-minute exposure; 3 – twelve-minute exposure.

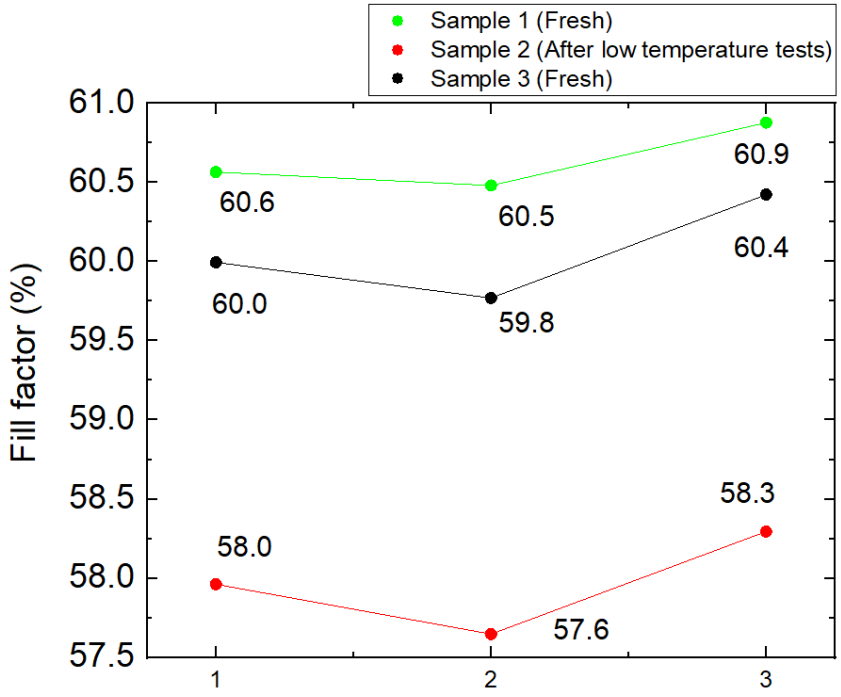

Fig. 24. Changes of Fill factor of three crystalsol CZTS cells after UV exposure; 1 – Initial; 2 – five-minute exposure; 3 – twelve-minute exposure.

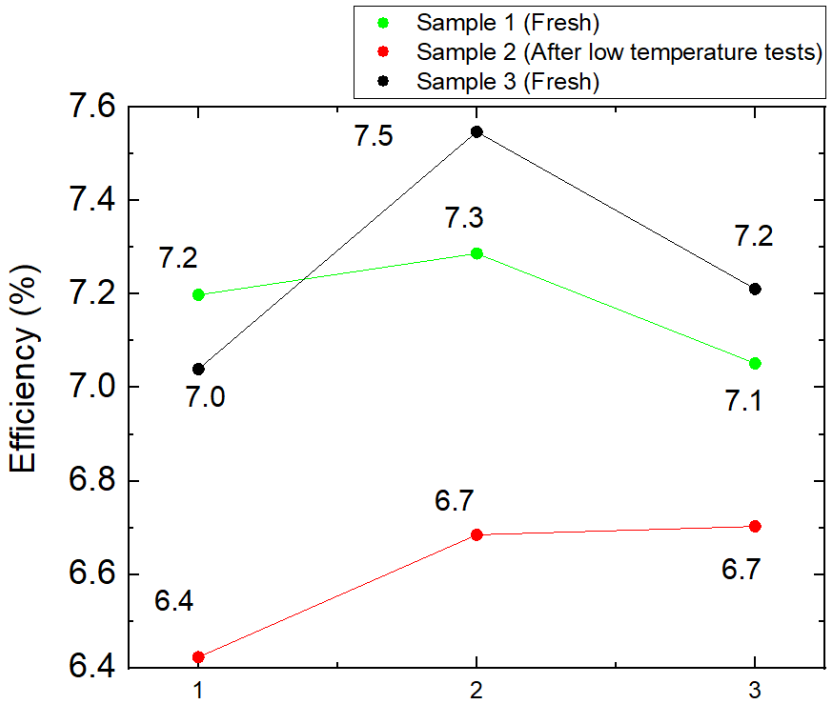

Fig. 25. Changes in the efficiency of three crystalsol CZTS cells before and after UV exposure; 1 – Initial; 2 – five-minute exposure; 3 – twelve-minute exposure.

It is important to note that the samples provided by crystalsol had been manufactured on a cover glass, which was a very important factor during ultraviolet measurements, due to the possibly limited transmittance of the cover glass. However, the graphical representation of the transmittance of the cover glass shown in the Figure 26, along with the spectrum of the lamp in Figure 21, show that enough portion of the ultraviolet radiation would go through (98%Transmittance at 360nm).

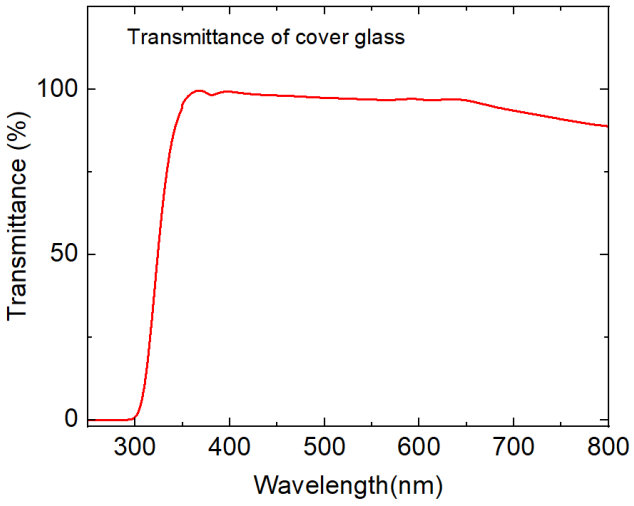

Fig. 26. Transmittance of the cover glass.

2.4. Thermal cycling tests

Objects in space are generally subject to extreme temperature cycles which can have a serious impact on the materials and components due constant thermal expansion and contraction. Particularly in the case of the lunar surface, depending on the exact location, the temperature might range from 127°C when fully exposed to the Sun to -173°C during the eclipse (Much lower temperatures have also been detected around the poles of the Moon). Combined with other environmental hazards, such as different kinds of radiation, severe thermal cycling of this extent can lead to a wide range of damage to the device on microscopic as well as macroscopic levels. Thermal tests are, therefore, required to prove the system's capability within the expected temperature range of the upcoming missions.

NASA has put forward several papers describing the thermal cycling tests and results for different solar cells. [64]discusses the simulated thermal cycle testing of BSFR (Back surface field reflected) silicon solar cells present on the rollup wings of the Hubble space telescope. Performance of these cells is assessed for 30,000 thermal cycles, in vacuum under simulated orbital conditions. For this test, the cycle limit temperature was limited to +75°C and -90°C. Different amount of cycles are conducted and the samples are visually and electrically characterized and assed after each one. The results do not show any serious signs of the degradations of the samples – Visual or electrical. The graphical representation of the main electrical parameters throughout the experiment can be seen in the figure below:

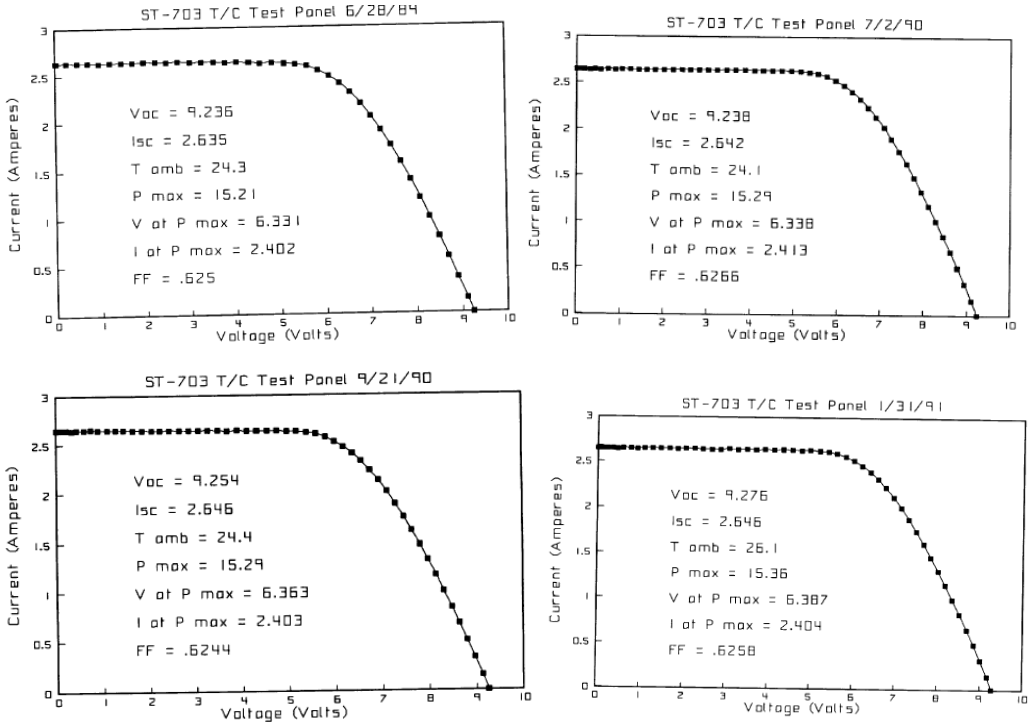

Fig. 27. Electrical performance of the modules initially and after 16,761, 22,469, 30,000 tests[64].

Similar experiment on thermal cycling of Mir Cooperative Solar Array[65] is described by [66]. After 24,000 thermal cycles between +80°C and -100°C, the authors report the degradation of the electrical performance of the samples only at elevated temperatures, partially explained by the loss in the cell area [67]. The graphical representation for the degradation mentioned above can be seen below:

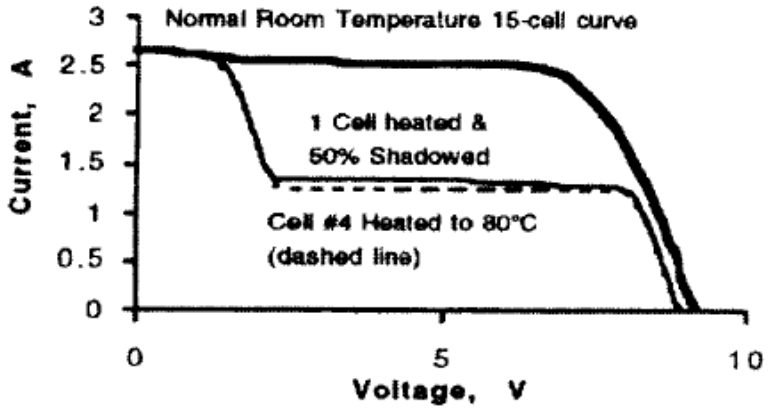

Fig. 28. IV curve for the 15 – cell series connected thermal cycle test[66].

Gallium arsenide (GaAs) have been tested as well for thermal stress cycling. As in the case of previous reports, the cycling was performed under low earth orbit simulated temperature conditions in vacuum. In this case 15,000 thermal cycles have been conducted with the temperature gradient of -80°C to +80°C. Interestingly, the authors report no electrical, mechanical and structural integrity degradation in this case as well (Results for solar cells alone, without interconnects and coverglass) [67].

2.4.1. Experimental procedure and results to date

To simulate somewhat extreme conditions of the lunar surface, the experiment temperature values were set at +125°C and -196°C. A furnace and liquid nitrogen were used for these respectively. The experimental procedure was conducted in 4 cycles – Submergence of the sample in liquid nitrogen for one minute; Submergence of the sample into liquid nitrogen for one minute followed by immediate furnace treatment for three minutes; Furnace treatment for ten minutes followed by immediate submergence into liquid nitrogen; Furnace treatment for thirty minutes followed by room temperature water followed by submergence into liquid

nitrogen; The sample was visually and electrically inspected after every cycle. The graphical representation of the electrical parameters can be seen below.

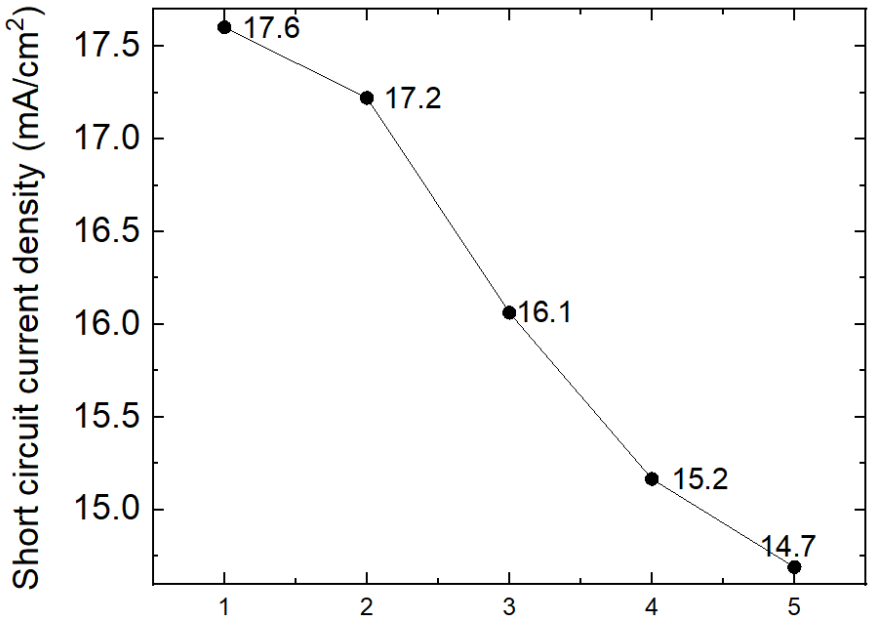

Fig. 29. Thermal cycling induced changes of short circuit current density.

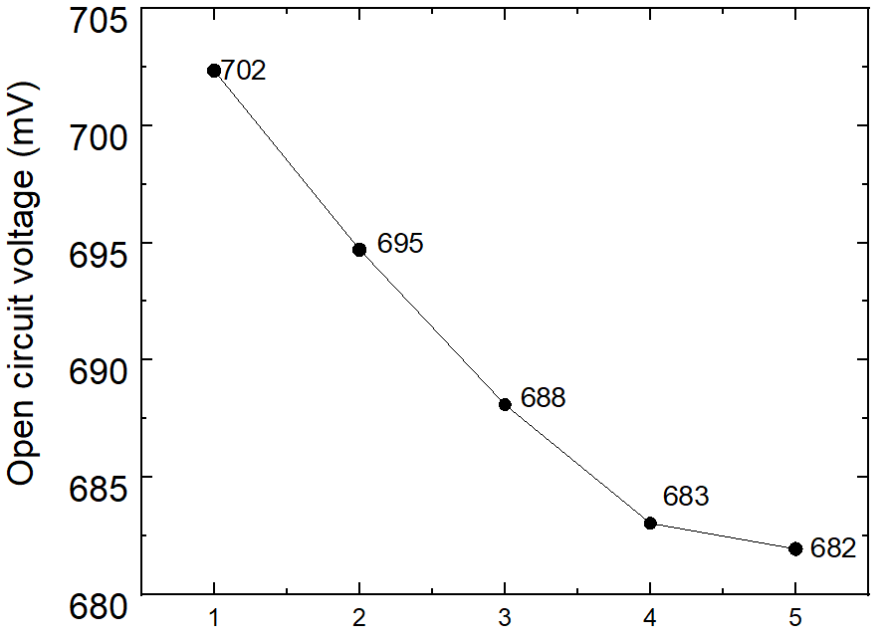

Fig. 30. Thermal cycling induced changes of open circuit voltage.

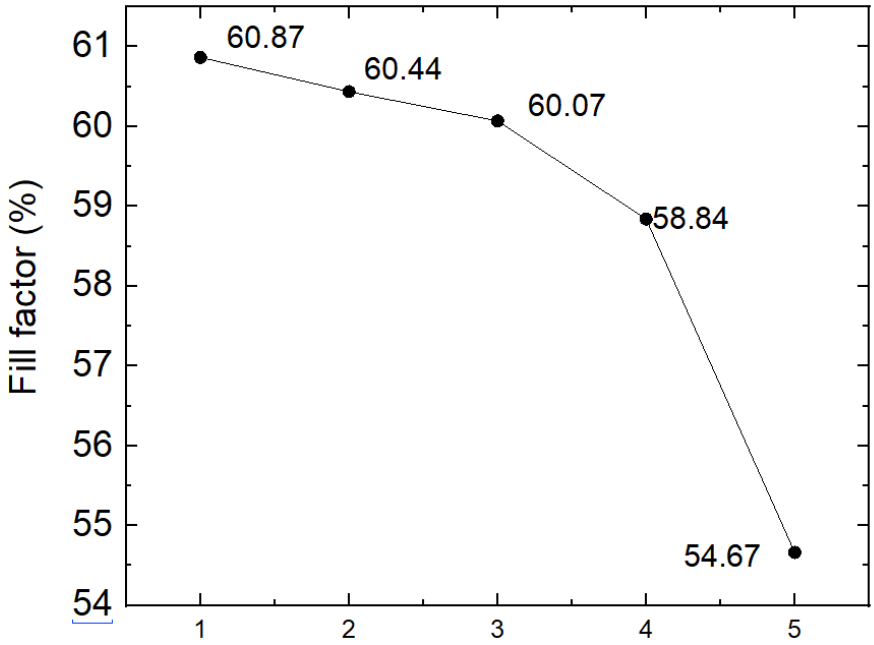

Fig. 31. Thermal cycling induced changes of fill factor.

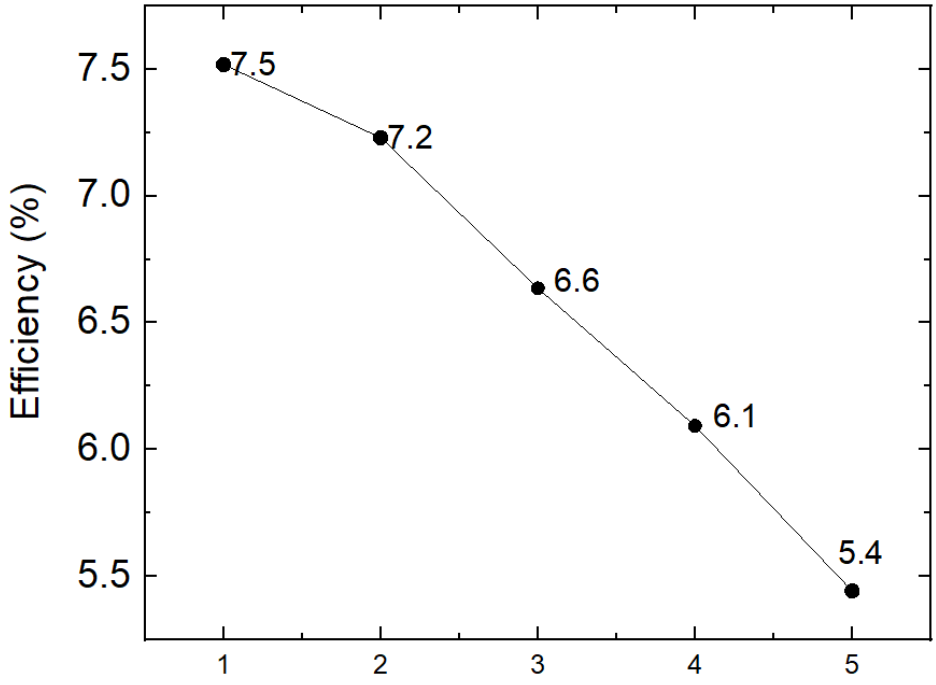

Fig. 32. Thermal cycling induced changes of efficiency.

As thermal cycling would cause tremendous mechanical stress for the components of the device due to continuous rapid thermal expansion and compression, it was sensible to contemplate the mechanical stability and integrity of the cell using scanning electron microscopy as well as visual inspection. On a macroscopic level the cracks in the coverglass

were visible towards the last thermal cycles, resulting in a total separation of the device after a slight impact. The microscopic changes, if any, can be seen in the figure below, where a brand-new cell is compared with the one used in thermal cycling tests. The are no visual signs of damage to the device, however consistent degradation in the performance is observed. Back and front contacts can be assumed to be the main mechanisms of degradation during thermal cycling.

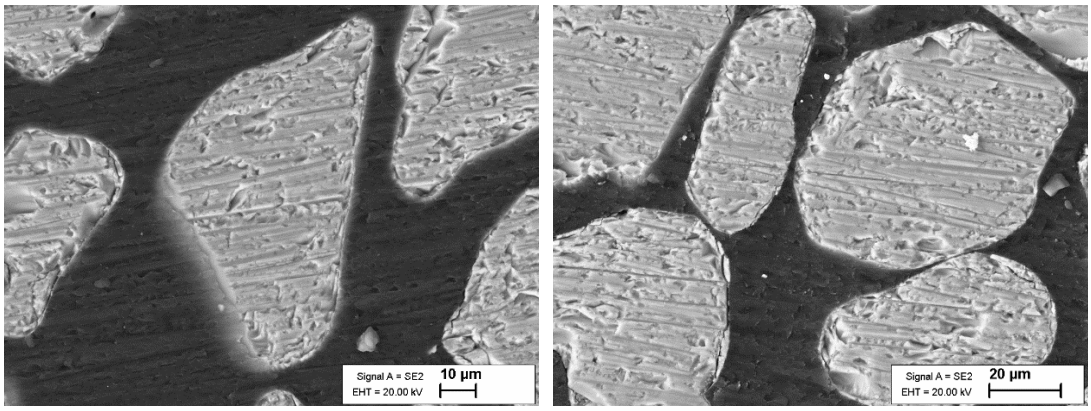

Fig. 33. SEM images of new (left) and tested (right) solar cells.

Conclusion

Detailed analyses has been carried out to test the performance of crystalsol's monograin CZTSSe photovoltaic cells in the lunar environment. An extensive, multidisciplinary research has been conducted to create the theoretical basis for the experimental procedure. As this kind of absorber material has hardly ever been considered in frames of extraterrestrial use before, let alone testing, the literature was reviewed for any similar papers concerning different, well- studied and understood materials like crystalline silicon and gallium arsenide. The behavior characteristics of these under different environmental aspects (Temperature dependence; Radiation; Thermal cycling) have been studied and presented according to different papers and publications by NASA, et.al.

Considering that the standard tests and systematic methods for verifying the usability of a device in extraterrestrial environment is quite extensive and diverse, the experimental procedure in the context of this thesis has been adopted available machinery and testing facilities. Particularly, photovoltaic devices have been tested for vacuum, low temperature, high temperature, ultraviolet radiation and thermal cycling.

Results to date have clearly shown the degradation trends of CZTSSe photovoltaic devices during the tests mentioned above. It should be noted, that most of the results acquired directly follow the theoretical formulation defined prior to every experiment. Namely:

1. Vacuum tests, mainly intended to verify the reliable mechanical integration and encapsulation of the devices, show no signs of negative effects on the cells' performance. Notably, minute increase in fill factor and efficiency values are observed.
2. Low temperature tests, intended to simulate the cold extreme of the lunar environment, have been conducted in vacuum over the temperature range of 320K – 20K. As expected, the devices maintain the characteristic solar cell behavior with continuous decrease in short circuit current, fill factor and efficiency values and a rapid increase in the open circuit voltage value.
3. Ultraviolet radiation tests, intended to simulate this specific type of radiation exposure in the open space, have been conducted using a mercury lamp with irradiation of 38 mW/cm^2. Interestingly, contrary to the literature, all the measurements taken (3 samples per 4 contacts each) demonstrated increase in the output parameters after the first, five-minute exposure to the ultraviolet radiation environment. Throughout the literature, similar behavior has also been noticed with a CIGS solar cells explained by neutralizing deep acceptor defects in the absorber near the interface. It is important to note, however, that this phenomenon was unique to the very first shorter exposure – the consecutive measurements after following,

longer exposures revealed the expected degradation trend of the cells with the increasing dose of radiation.

4. Thermal cycling tests, intended to simulate the huge temperature gradients of the lunar environment, have been conducted by means of submerging the samples in liquid nitrogen to afterwards be subject to 125°C furnace for a certain period for certain amount of cycles. After the measurements the cells demonstrated a persistent decrease in all the electrical parameters, especially after exposure to extremely hot environment. It should be noted, however, that the temperature values, especially the one provided by liquid nitrogen, were set to almost unrealistic extremes to lunar conditions. Also, the transition from low temperature to high temperature during the experimental procedure was almost immediate, which is highly unlikely in the real environment, where the cycling would be gradual.

According to the results available at present, under the particular conditions that were studied in frames of this thesis, crystalsol's CZTSSe monograin solar cells demonstrate theoretically predictable behavior for the most part. Vacuum, low temperature, high temperature and thermal cycling tests showed well-defined trends in the induced changes in accordance with prior theoretical formulation. Ultraviolet radiation tests, in turn, gave relatively unconventional results, by consistently inducing increase in the electrical parameters of the solar cell after the first exposure.

It should be mentioned, however, that ordinary samples, intended for terrestrial application, were used. However, they showed good resistance to degradation during the experimental procedure, which makes this topic worth elaborating and further investigating in the future. As these were in no way prepared for extraterrestrial conditions, it is sensible to deduce that superior performance shall be expected given the devices are prepared accordingly (Proper encapsulation; Proper material choice for the device components – substrate, polymer, contacts).

[1] P. A. Iles, “Evolution of space solar cells,” 2001.

[2] S. Loff, “Vanguard Satellite, 1958,” 2015, Accessed: May 09, 2020. [Online].

[3] U.S Department of Energy“solar_timeline.”

[4] J. Blosiu *et al.*, “Solar Power Technologies for Future Planetary Science Missions Work Performed under the Planetary Science Program Support Task Advisory Committee and Editors,” 2017. [Online]. Available: https://solarsystem.nasa.gov.

[5] T. v Torchynska and G. Polupan, “High efficiency solar cells for space applications,” 2004.

[6] V. M. Andreev, “GaAs and High-Cells Efficiency Space 1 Historical Review of III-V Solar Cells 2 Single-Junction III-V Space Solar Cells 2.1 Solar Cells Based on A1GaAs/GaAs Structures 2.2 Solar Cells With Internal Bragg Reflector 2.3 GaAs-Based Cells on Ge Substrates 3 Multi-junction Space Solar Cells 3.1 Mechanically Stacked Cells 3.2 Monolithic Multi-junction Solar Cells Acknowledgements References.”

[7] “Novel solar cells arrive at International Space Station for testing.” https://techxplore.com/news/2019-11-solar-cells-international-space-station.html (accessed May 09, 2020).

[8] “Material Samples to be Tested on the International Space Station | NASA.” https://www.nasa.gov/centers/armstrong/features/misse-11.html (accessed May 09, 2020).

[9] M. Conner, “Material Samples to be Tested on the International Space Station,” 2018, Accessed: May 09, 2020. [Online].

[10] “Tech Xplore | Georgia Institute of Technology.” https://techxplore.com/partners/georgia-institute-of-technology/ (accessed May 09, 2020).

[11] C. Warner, “NASA’s Lunar Outpost will Extend Human Presence in Deep Space,” 2018, Accessed: May 09, 2020. [Online].

[12] “NASA’s Lunar Outpost will Extend Human Presence in Deep Space | NASA.” https://www.nasa.gov/feature/nasa-s-lunar-outpost-will-extend-human-presence-in-deep-space (accessed May 09, 2020).

[13] H. Benaroya and L. Bernold, “Engineering of lunar bases,” *Acta Astronautica*, vol. 62, no. 4–5. pp. 277–299, Feb. 2008, doi: 10.1016/j.actaastro.2007.05.001.

[14] R. D. Johnson, “Space Settlements A Design Study Edited by.”

[15] H. Benaroya, ; Leonhard Bernold, M. Asce, K. M. Chua, and F. Asce, “Engineering, Design and Construction of Lunar Bases,” doi: 10.1061/ASCE0893-1321200215:233.

[16] M. P. Suryawanshi *et al.*, “CZTS based thin film solar cells: A status review,” *Materials Technology*, vol. 28, no. 1–2. pp. 98–109, Mar. 2013, doi: 10.1179/1753555712Y.0000000038.

[17] East-West University, Institute of Electrical and Electronics Engineers, Institute of Electrical and Electronics Engineers. Bangladesh Section, and IEEE Robotics and Automation Society. Bangladesh Chapter, *2019 1st International Conference on Advances in Science, Engineering and Robotics Technology (ICASERT 2019) : May 3-5, 2019, Dhaka, Bangladesh.* .

[18] A. Khare, B. Himmetoglu, M. Johnson, D. J. Norris, M. Cococcioni, and E. S. Aydil, “Calculation of the lattice dynamics and Raman spectra of copper zinc tin chalcogenides and comparison to experiments,” *Journal of Applied Physics*, vol. 111, no. 8, Apr. 2012, doi: 10.1063/1.4704191.

[19] H. Katagiri, N. Sasaguchi, S. Hando, S. Hoshino, J. Ohashi, and T. Yokota, “Preparation films by and evaluation of Cu2ZnSnS4 thin sulfurization of E-B evaporated precursors,” 1997.

[20] C. Yan *et al.*, “Cu2ZnSnS4 solar cells with over 10% power conversion efficiency enabled by heterojunction heat treatment,” *Nature Energy*, vol. 3, no. 9, pp. 764–772, Sep. 2018, doi: 10.1038/s41560-018-0206-0.

[21] Y. S. Lee *et al.*, “Cu2ZnSnSe4 thin-film solar cells by thermal co-evaporation with 11.6% efficiency and improved minority carrier diffusion length,” *Advanced Energy Materials*, vol. 5, no. 7, Apr. 2015, doi: 10.1002/aenm.201401372.

[22] W. Wang *et al.*, “Device characteristics of CZTSSe thin-film solar cells with 12.6% efficiency,” *Advanced Energy Materials*, vol. 4, no. 7, May 2014, doi: 10.1002/aenm.201301465.

[23] M. A. Green *et al.*, “Solar cell efficiency tables (Version 53),” *Progress in Photovoltaics: Research and Applications*, vol. 27, no. 1, pp. 3–12, Jan. 2019, doi: 10.1002/pip.3102.

[24] C. Oü, “EXECUTIVE SUMMARY REPORT ESR Project: ‘crystalsol Solar Panel Technology for Space Applications’ ESA Contract No. 4000125757/18/NL/CBi,” 2019.

[25] “Moon Fact Sheet.” https://nssdc.gsfc.nasa.gov/planetary/factsheet/moonfact.html (accessed May 09, 2020).

[26] F. S. Johnson, J. M. Carroll, and D. E. Evans, “Vacuum Measurements on the Lunar Surface,” *Journal of Vacuum Science and Technology*, vol. 9, no. 1, pp. 450–456, Jan. 1972, doi: 10.1116/1.1316652.

[27] “LUNAR RECONNAISSANCE ORBITER: Temperature Variation on the Moon North Pole Maximum Temperature Minimum Temperature.” Accessed: May 09, 2020. [Online]. Available: www.nasa.gov.

[28] G. Reitz, T. Berger, and D. Matthiae, “Radiation exposure in the moon environment,” in *Planetary and Space Science*, Dec. 2012, vol. 74, no. 1, pp. 78–83, doi: 10.1016/j.pss.2012.07.014.

[29] “By the Numbers | Earth’s Moon – NASA Solar System Exploration.” https://solarsystem.nasa.gov/moons/earths-moon/by-the-numbers/ (accessed May 09, 2020).

[30] M. Yamaguchi, “Radiation-resistant solar cells for space use.”

[31] P. A. Iles F Ho, M. Yeh, G. Datum, and S. Billets, “GALLIUM ARSENIDE-ON-GERMANIUM SOLAR CELLS.”

[32] “(No Title).” https://www.nrel.gov/pv/assets/pdfs/best-research-cell-efficiencies.20200406.pdf (accessed May 17, 2020).

[33] R. K. Jones, J. H. Ermer, C. M. Fetzer, and R. R. King, “Evolution of multijunction solar cell technology for concentrating photovoltaics,” *Japanese Journal of Applied Physics*, vol. 51, no. 10 PART 2, Oct. 2012, doi: 10.1143/JJAP.51.10ND01.

[34] P. Sharps *et al.*, “NEXT GENERATION RADIATION HARD IMM SPACE SOLAR CELLS.”

[35] D. McCamey, “An Upside-Down Solar Cell Achieves Record Efficiencies (Fact Sheet), The Spectrum of Clean Energy Innovation, NREL (National Renewable Energy Laboratory),” 2005. [Online]. Available: www.nrel.gov.

[36] I. Garcia *et al.*, “Metamorphic III-V solar cells: Recent progress and potential,” *IEEE Journal of Photovoltaics*, vol. 6, no. 1, pp. 366–373, Jan. 2016, doi: 10.1109/JPHOTOV.2015.2501722.

[37] A. Duda, S. Ward, and M. Young, “Inverted Metamorphic Multijunction (IMM) Cell Processing Instructions,” 2012. [Online]. Available: http://www.osti.gov/bridge.

[38] A. Aho, R. Isoaho, A. Tukiainen, G. Gori, R. Campesato, and M. Guina, “Dilute nitride triple junction solar cells for space applications: Progress towards highest AM0 efficiency,” *Progress in Photovoltaics: Research and Applications*, vol. 26, no. 9, pp. 740–744, Sep. 2018, doi: 10.1002/pip.3011.

[39] E3S Web of Conferences 16, 03006 (2017)

[40] J. M. Zahler *et al.*, “Wafer bonding and layer transfer processes for 4-junction high efficiency solar cells,” in *Conference Record of the IEEE Photovoltaic Specialists Conference*, 2002, pp. 1039–1042, doi: 10.1109/pvsc.2002.1190783.

[41] G. A. Landis and M. A. Perino, “Lunar Production of Solar Cells.” [Online]. Available: https://ntrs.nasa.gov/search.jsp?R=19890018248.

[42] “AIAA S-111A-201X Standard Qualification and Quality Requirements for Space Solar Cells,” 2014.

[43] “IV Curve | PVEducation.” https://www.pveducation.org/pvcdrom/solar-cell-operation/iv-curve (accessed May 26, 2020).

[44] P. Singh and N. M. Ravindra, “Temperature dependence of solar cell performance - An analysis,” *Solar Energy Materials and Solar Cells*, vol. 101, pp. 36–45, Jun. 2012, doi: 10.1016/j.solmat.2012.02.019.

[45] M. Altosaar *et al.*, “Monograin layer solar cells,” in *Thin Solid Films*, May 2003, vol. 431–432, pp. 466–469, doi: 10.1016/S0040-6090(03)00167-6.

[46] “290 Copper Zinc Tin Sulfide-Based Thin-Film Solar Cells.”

[47] “Company presentation,” 2017.

[48] C. Oü, “Project: ‘crystalsol Solar Panel Technology for Space Applications’ ESA Contract No. 4000125757/18/NL/CBi,” 2019.

[49] T. Raadik, “" Adapting CRYSTALSOL Product to a Moon Environment ",” 2016.

[50] C. Neubauer, *Spatially Resolved Opto-electronical Investigations of Monograin Layer Solar Cells*. .

[51] M. A. Green, “General temperature dependence of solar cell performance and implications for device modelling,” *Progress in Photovoltaics: Research and Applications*, vol. 11, no. 5, pp. 333–340, Aug. 2003, doi: 10.1002/pip.496.

[52] B. S. Phillips, T. A. Schneider, J. A. Vaughn, and K. H. Wright, “Space Environment Testing of Photovoltaic Array Systems at NASA’s Marshall Space Flight Center.” [Online]. Available: https://ntrs.nasa.gov/search.jsp?R=20150022334.

[53] B. E. Anspaugh, “GaAs Solar Cell Radiation Handbook,” 1996. [Online]. Available: https://ntrs.nasa.gov/search.jsp?R=19970010878.

[54] M. Tayyib, J. O. Odden, and T. O. Saetre, “UV-induced degradation study of multicrystalline silicon solar cells made from different silicon materials,” in *Energy Procedia*, 2013, vol. 38, pp. 626–635, doi: 10.1016/j.egypro.2013.07.326.

[55] F. U. Hamelmann, J. A. Weicht, and G. Behrens, “Light-Induced Degradation of Thin Film Silicon Solar Cells,” in *Journal of Physics: Conference Series*, Feb. 2016, vol. 682, no. 1, doi: 10.1088/1742-6596/682/1/012002.

[56] P. Bhushan Sopori *et al.*, “Understanding Light-Induced Degradation of c-Si Solar Cells: Preprint,” 2012. [Online]. Available: http://www.osti.gov/bridge.

[57] J. Lindroos and H. Savin, “Review of light-induced degradation in crystalline silicon solar cells,” *Solar Energy Materials and Solar Cells*, vol. 147. Elsevier, pp. 115–126, Apr. 01, 2016, doi: 10.1016/j.solmat.2015.11.047.

[58] L. Dunn, M. Gostein, and B. Stueve, “Literature Review of the Effects of UV ! Exposure on PV Modules ! !,” 2013. Accessed: May 26, 2020. [Online]. Available: www.atonometrics.com!

[59] L. Dunn, M. Gostein, and B. Stueve, “Literature Review of the Effects of UV ! Exposure on PV Modules ! !,” 2013. [Online]. Available: www.atonometrics.com!

[60] C. R. Osterwald, J. Pruett, and T. Moriarty, “Crystalline Silicon Short-Circuit Current Degradation Study: Initial Results,” 2005. [Online]. Available: http://www.osti.gov/bridge.

[61] N. Rolston, A. D. Printz, S. R. Dupont, E. Voroshazi, and R. H. Dauskardt, “Effect of heat, UV radiation, and moisture on the decohesion kinetics of inverted organic solar cells,” *Solar Energy Materials and Solar Cells*, vol. 170, pp. 239–245, Oct. 2017, doi: 10.1016/j.solmat.2017.06.002.

[62] S. W. Lee *et al.*, “UV Degradation and Recovery of Perovskite Solar Cells,” *Scientific Reports*, vol. 6, Dec. 2016, doi: 10.1038/srep38150.

[63] H. J. Yu *et al.*, “Light-soaking effects and capacitance profiling in Cu(In,Ga)Se2 thin-film solar cells with chemical-bath-deposited ZnS buffer layers,” *Physical Chemistry Chemical Physics*, vol. 18, no. 48, pp. 33211–33217, Dec. 2016, doi: 10.1039/c6cp05306h.

[64] D. W. Alexander, “HUBBLE SPACE TELESCOPE THERMAL CYCLE TEST REPORT FOR LARGE SOLAR ARRAY SAMPLES WITH BSFR CELLS (Sample Numbers 703 and 704),” 1992. [Online]. Available: https://ntrs.nasa.gov/search.jsp?R=19930001621.

[65] “Mir Cooperative Solar Array.” Accessed: May 10, 2020. [Online]. Available: https://ntrs.nasa.gov/search.jsp?R=20050177155.

[66] D. J. Hoffman, D. A. Scheiman, by AIChE, and I. Honolulu, “Thermal Cycling of Mir Cooperative Solar Array (MCSA) Test Panels.” [Online]. Available: https://ntrs.nasa.gov/search.jsp?R=19970028356.

[67] R. W. Francis, “THERMAL STRESS CYCLING OF GaAs SOLAR CELLS.” [Online]. Available: https://ntrs.nasa.gov/search.jsp?R=19870016985.